Radiative muon capture by ^{3}He

Ernest C. Y. Ho
Department of Physics and Astronomy, University of British Columbia, 6224 Agricultural Road, Vancouver, British Columbia, Canada V6T 1Z1

Harold W. Fearing and Wolfgang Schadow*
TRIUMF, 4004 Wesbrook Mall, Vancouver, British Columbia, Canada V6T 2A3

(Received 11 December 2001; published 10 June 2002)

The rate of the nuclear reaction $^3\mathrm{He}+\mu^-\rightarrow{}^3\mathrm{H}+\gamma+\nu_\mu$ has been calculated using both the elementary particle model (EPM) approach and the impulse approximation (IA) approach. Using the EPM approach, the exclusive statistical radiative muon capture (RMC) rate for photon energy greater than 57 MeV is found to be 0.245 s^{-1} and the ordinary muon capture (OMC) rate is found to be 1503 s^{-1}. The IA calculation exhibits a slight dependence on the type of trinucleon wave functions used. The difference between the IA and EPM calculation is larger for RMC than for OMC. To resolve the difference between the two approaches, a more detailed investigation including meson exchange corrections will be required.

DOI: 10.1103/PhysRevC.65.065501 PACS number(s): 23.40.−s, 21.45.+v, 13.10.+q, 24.80.+y

I. INTRODUCTION

A recent TRIUMF experiment [1,2] designed to measure the rate of the radiative muon capture (RMC) reaction $^3\mathrm{He}+\mu^-\rightarrow{}^3\mathrm{H}+\gamma+\nu_\mu$ has sparked a renewed interest in this process. Since it is more sensitive to the nucleon pseudoscalar form factor g_P than its nonradiative counterpart (Refs. [3,4] are two reviews on ordinary muon capture), it is an ideal candidate for checking the value of this form factor, which is theoretically predicted by PCAC (partial conservation of axial current). With the experiment going on, it is necessary to have a modern theoretical calculation of the process to interpret the anticipated experimental results. In this paper, we have calculated the rate of the process using two perspectives: a nuclear perspective via the elementary particle model (EPM) and a nucleon perspective via the impulse approximation (IA).

The only similar calculation for this process was done by Klieb and Rood [5,6] about 20 years ago but the accuracy of their calculation is constrained by the facts that (1) the trinucleon wave function they used is inadequate by today's standards, (2) some of the nucleon momentum terms were handled in an approximate way, and (3) they did not use the full Adler and Dothan amplitude but included only some of the Adler and Dothan terms. As a consequence of better computer technology and better methods of calculation of realistic trinucleon wave functions, it has been possible in this calculation to improve on the approximations they made. The analogous nonradiative, or ordinary muon capture (OMC), reaction has been considered by several authors. See, for example, Refs. [7–10] and references cited therein.

In Sec. II we will briefly discuss various hypotheses governing the weak hadronic current and the Adler and Dothan [11] procedure, which provides terms in addition to the terms generated by a naive insertion of photons on each particle with charge or magnetic moment (see also Ref. [12] for early work on this topic and Ref. [13] for an alternative presentation of the Adler and Dothan procedure). The elementary particle model approach is discussed in Sec. III, where both ^{3}He and ^{3}H nuclei are treated as single entities with internal structure revealed only by the phenomenological nuclear form factors taken from experiments. We will then discuss the impulse approximation approach in Sec. IV. The essence of the impulse approximation is that it regards the radiative capture process as taking place on the constituent nucleons. Assuming that the nucleons are free, one then uses a trinucleon wave function to integrate out the internal degrees of freedom. The resulting amplitude will be one that only depends on the EPM, or external degrees of freedom. The results will be presented in Sec. V and a summary in Sec. VI.

II. THE TRANSITION AMPLITUDE

The fundamental terms of the transition amplitude are obtained by inserting a photon on all particles carrying charge or magnetic moment. Figure 1 shows the Feynman diagrams corresponding to these terms. Note that this general approach is common to both EPM and IA so that the form of the transition amplitude derived here will be applied to the nucleus in the EPM, but to the nucleon in the IA.

The amplitudes corresponding to the diagrams in Fig. 1 are

$$M_1=\overline{u}(\nu)\gamma_\alpha(1-\gamma^5)u(\mu)\times\overline{u}(P_f)W^\alpha(Q^H)S_F(P_i-k)\mathcal{Q}_i u(P_i),$$

$$M_2=\overline{u}(\nu)\gamma_\alpha(1-\gamma^5)u(\mu)\times\overline{u}(P_f)\mathcal{Q}_f S_F(P_f+k)W^\alpha(Q^H)u(P_i),$$

*Present address: Cap Gemini Ernst and Young, Hamborner Str. 55, D-40472 Düsseldorf, Germany.

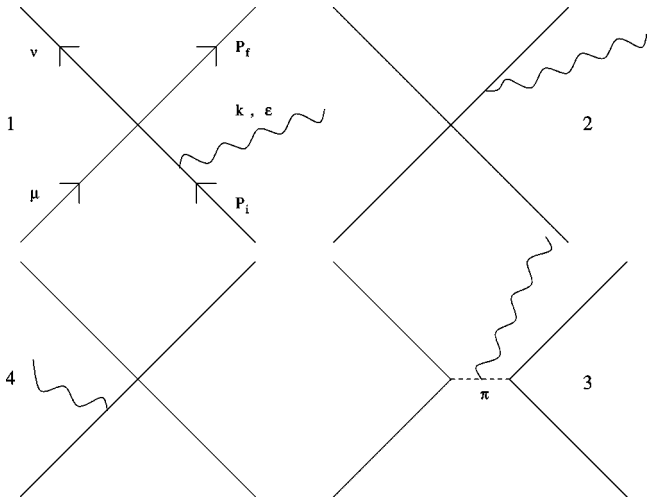

FIG. 1. The fundamental radiating diagrams.

$$M_3=\overline{u}(\nu)\gamma_\alpha(1-\gamma^5)u(\mu)$$
$$\times\overline{u}(P_f)\left\{\frac{-i}{m_\pi^2-(Q^H-k)^2}(-i)(2Q^H-k)\cdot\epsilon G_P^H\right\}$$
$$\times\frac{Q_H^\alpha}{m}\gamma^5 u(P_i),$$

$$M_4=\overline{u}(\nu)\gamma_\alpha(1-\gamma^5)S_F(\mu-k)(-i\not\epsilon)u(\mu)$$
$$\times\overline{u}(P_f)W^\alpha(Q^L)u(P_i), \tag{1}$$

where S_F is the Feynman propagator for spin $\frac{1}{2}$ particles ($S_F(P_i-k)=i/(\not P_i-\not k-M_n)$, for example), ν, μ, and k are the four-momenta of the neutrino, muon, and emitted photon, respectively, and $W^\alpha(Q)$ is the weak hadronic vertex, which is parametrized by four form factors

$$W^\alpha(Q)=G_V\gamma^\alpha+G_M i\sigma^{\alpha\beta}\frac{Q_\beta}{2M_n}+G_A\gamma^\alpha\gamma^5+G_P\gamma^5\frac{Q^\alpha}{m}, \tag{2}$$

$$\sigma^{\alpha\beta}\equiv\frac{i}{2}(\gamma^\alpha\gamma^\beta-\gamma^\beta\gamma^\alpha) \tag{3}$$

with all the G_i's being functions of Q^2, the square of the momentum transfer at the weak hadronic vertex. Specifically, we denote $Q^H=\mu-\nu$ as the momentum transfer at the hadronic vertex when one of the hadrons is radiating and $Q^L=\mu-\nu-k$ as the momentum transfer when the lepton is radiating. $\mathcal{Q}_{i(f)}=ie_{i(f)}\not\epsilon+[\kappa_{i(f)}/2M_n]\sigma^{\lambda\rho}k_\rho\epsilon_\lambda$, where $e_i(e_f)$, $\kappa_i(\kappa_f)$ denote the electric charge and anomalous magnetic moment of the initial (final) particle. The induced pseudoscalar coupling G_P, which originates from the pion pole term has the form [14]

$$G_P(Q^2)=\frac{2mM_nG_A(Q^2)(1+\varepsilon)}{m_\pi^2-Q^2}$$
$$\varepsilon=\frac{m_\pi^2}{-Q^2}\left\{1-\frac{G_\pi(Q^2)/G_\pi(0)}{G_A(Q^2)/G_A(0)}\right\} \tag{4}$$

which comes from PCAC and the Goldberger-Treiman relation for ordinary muon capture. The quantity ε can be regarded as a constant over the Q^2 concerned [5–8]. The PCAC value of G_P is defined as $\varepsilon=0$. G_π is the pion-i-f coupling constant. In the EPM, the hadronic vertex is at the nuclear level. Therefore, $P_i\equiv P_{^3\mathrm{He}}$ (four-momentum of the ^{3}He nucleus) and $P_f\equiv P_{^3\mathrm{H}}$ (four-momentum of the ^{3}H nucleus). In the IA, the hadronic weak interaction operator acts on the constituent *nucleons* and so $P_i\equiv p$ (four-momentum of the proton) and $P_f\equiv n$ (four-momentum of the neutron). Note also that M_n is the mass of the nucleus in the EPM but the mass of the nucleon in the IA and m (m_π) is used to denote the mass of the muon (charged pion) throughout.

However, the sum of these four diagrams is not gauge invariant (GI) and does not satisfy conserved vector current (CVC) and PCAC by itself. Extra terms must be added in order for the whole transition amplitude to be gauge invariant and to satisfy CVC and PCAC up to a desired order. The Adler and Dothan procedure is used to generate these terms up to $\mathcal{O}(k^0)$ via the GI requirement and $\mathcal{O}(Q^0)$ via the CVC and PCAC hypotheses. The extra piece of amplitude that is required is

$$\Delta M=\Delta M_1+\Delta M_2+\Delta M_3, \tag{5}$$

$$\Delta M_1=-\overline{u}(\nu)\gamma_\alpha(1-\gamma^5)u(\mu)$$
$$\times\overline{u}(P_f)\left\{G_M^L i\sigma^{\alpha\zeta}\frac{\epsilon_\zeta}{2M_n}+G_P^L\frac{\epsilon_\alpha}{m}\gamma^5\right\}u(P_i), \tag{6}$$

$$\Delta M_2=\overline{u}(\nu)\gamma_\alpha(1-\gamma^5)u(\mu)$$
$$\times\overline{u}(P_f)\left\{-2(G_V'\gamma_\mu+G_A'\gamma_\mu\gamma^5)(k^\alpha\epsilon^\mu-k^\mu\epsilon^\alpha)\right.$$
$$\left.-G_V'(\kappa_f-\kappa_i)\frac{2k^\alpha}{2M_n}i\sigma^{\beta\zeta}k_\zeta\epsilon_\beta\right\}u(P_i), \tag{7}$$

$$\Delta M_3=\overline{u}(\nu)\gamma_\alpha(1-\gamma^5)u(\mu)$$
$$\times\overline{u}(P_f)\left\{-2(G_V'\gamma_\mu+G_A'\gamma_\mu\gamma^5)g^{\mu\alpha}Q^H\cdot\epsilon\right.$$
$$-\frac{2mM_nG_A'(1+\varepsilon)}{m_\pi^2-Q_L^2}\frac{2Q^H\cdot\epsilon}{m}Q_H^\alpha\gamma^5$$
$$\left.-G_M'i\sigma^{\alpha\beta}\frac{Q^H{}_\beta}{2M_n}(2Q^H\cdot\epsilon)\right\}u(P_i). \tag{8}$$

A prime on a form factor denotes the derivative with respect to Q^2. Since all the form factors (except G_P, which contains a pole term) are almost linear in Q^2 over the range of Q^2 concerned in both the EPM and IA, it does not matter with respect to which Q^2 the derivative is taken. The pion pole terms of G_P are treated exactly.

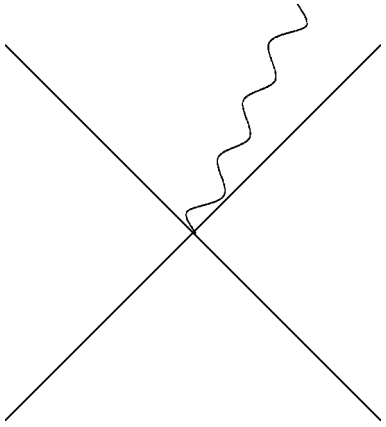

FIG. 2. The ''minimal coupling'' diagram.

The term ΔM_1 in ΔM arises when one does a minimal substitution on the hadronic vertex, assuming constant form factors, and corresponds to the usual fifth diagram included in previous RMC calculations (Fig. 2). If the nuclei or nucleons were elementary particles with no form factors, this would be the only term needed in ΔM in order to ensure GI, CVC, and PCAC of the amplitude. The other terms in ΔM involving derivatives of form factors are the terms to account for the composite nature of both the nuclei (in the EPM) and the nucleons (in the IA). The term ΔM_2 is demanded by the CVC and PCAC while the terms in ΔM_3 are demanded by the gauge invariance requirement in the case when form factors are included.[1]

The full amplitude $M \equiv \Sigma_{i=1-4} M_i + \Delta M$ satisfies GI, CVC, and PCAC up to, but not including, terms of $\mathcal{O}(kQ)$ and this is the amplitude that we will use for later calculations.

III. THE ELEMENTARY PARTICLE MODEL

The *elementary particle model* is probably the simplest method to calculate the RMC rate. It was first used by Kim and Primakoff [15,16] in calculating the beta decay of complex nuclei and was subsequently used by Fearing [17] and Klieb and Rood [5,6] in their RMC calculations. In this approach, both the ^{3}He and ^{3}H are treated as ''elementary particles'' of spin $\frac{1}{2}$ and isospin $\frac{1}{2}$ up to a small isospin breaking. The details of the structure of the nuclei are encapsulated in the nuclear form factors, which are determined by experiments done on these nuclei. One of the major reasons the EPM calculation is easier than the IA is that there are many fewer degrees of freedom that one has to take care of in the EPM than in the IA. The degrees of freedom in the EPM approach are the four-momenta of ^{3}He ($P_{^3\mathrm{He}}$), ^{3}H ($P_{^3\mathrm{H}}$), photon (k), neutrino (ν), and muon (μ) together with their respective spins. The four-momentum conservation relation is

$$P_{^3\mathrm{H}} + \nu + k = P_{^3\mathrm{He}} + \mu. \tag{9}$$

The differential capture rate (photon spectrum) is given by

$$\frac{d\Gamma}{dk} = \sum_{\text{photon polarization}} \int \frac{d\mathcal{P}}{dk} \times \mathrm{Tr}[\rho M(P_{^3\mathrm{H}}, P_{^3\mathrm{He}}, M_t)^\dagger M(P_{^3\mathrm{H}}, P_{^3\mathrm{He}}, M_t)], \tag{10}$$

where $d\mathcal{P}$ is the differential phase space factor

$$d\mathcal{P} = C|\phi_\mu(0)|^2 \frac{|V_{ud}|^2 G_F^2}{2} \frac{d^3\vec{P}_{^3\mathrm{H}}}{(2\pi)^3} \frac{d^3\vec{\nu}}{(2\pi)^3} \frac{1}{k} \frac{d^3\vec{k}}{(2\pi)^3} \times (2\pi)^4 \delta^{(4)}(\mu + P_{^3\mathrm{He}} - P_{^3\mathrm{H}} - k - \nu)$$

$$= C|\phi_\mu(0)|^2 \frac{1}{2\pi^5} \frac{|V_{ud}|^2 G_F^2}{2} \frac{2P^0_{^3\mathrm{H}}}{k} |2k(1-\cos(\theta)) - 2(m+M_t)|^{-1} \nu^2(k,\theta) d\hat{\nu} k^2 dk d\hat{k}, \tag{11}$$

$$\cos(\theta) = \hat{\nu}\cdot\hat{k}, \tag{12}$$

$$\nu(k,\theta) = \frac{2k(m+M_t) - m^2 - 2mM_t}{2k(1-\cos(\theta)) - 2(m+M_t)}, \tag{13}$$

$$M_t = 2808.66 \ \text{MeV}. \tag{14}$$

Here $\phi_\mu(0)$ denotes the muon wave function at the origin, $C = 0.9788$ [7,8] is the correction factor that accounts for the nonpointlike nature of the nucleus, and V_{ud} is the CKM matrix element, which connects the up and down quark, with $|\mathrm{V}_{ud}| = 0.9735 \pm 0.0008$[19]. G_F is the Fermi coupling constant, ρ is the density matrix that describes the initial spin configuration of the muonic atom, and $M(P_{^3\mathrm{H}}, P_{^3\mathrm{He}}, M_t)$ is the transition amplitude M that was discussed in Sec. II with the following changes:

$$u(P_i) \to u(P_{^3\mathrm{He}}),$$

$$\overline{u}(P_f) \to \overline{u}(P_{^3\mathrm{H}}),$$

$$M_n \to M_t \ \text{on the hadronic vertex},$$

$$G_i \to F_i, \tag{15}$$

where $F_i, i = V, M, A$ are the nuclear form factors which are parametrized as

$$F_i = F_i(0)\left(1 + \frac{1}{6} R_i^2 Q^2\right) \tag{16}$$

with $F_V(0) = 1$, $R_V = 1.94$ fm [7], $F_M(0) = \kappa_{^3\mathrm{He}} - \kappa_{^3\mathrm{H}} = -8.369$ nm $- 7.913$ nm, $R_M = 1.72$ fm [7], $F_A(0) = 1.212 \pm 0.004$ [8], $R_A = 1.703$ fm [7].

The photon polarization vector $\vec{\epsilon}_\lambda$, which is defined by $\vec{\epsilon}_\lambda \equiv (1/\sqrt{2})(\hat{x} + i\lambda\hat{y})$, with $\hat{k} = \hat{z}$, has the property

[1]These are almost all the terms considered by Adler and Dothan [11], except that we have not considered the non-Born terms in the pion photoproduction amplitude, which are thought to be small. Klieb and Rood [5,6] did not have the last term in ΔM_2 and the last two terms in ΔM_3.

$$\vec{k}\times\vec{\epsilon}_\lambda = -i\lambda k\vec{\epsilon}_\lambda . \tag{17}$$

Thus the $\Sigma_{\text{photon polarization}}$ in Eq. (10) can be replaced by $\Sigma_{\lambda=-1,+1}$.

The big advantage of the EPM is its simplicity. It also includes, to some extent at least, part of the meson exchange corrections that are missing in the IA. It, however, does have a major flaw as applied to a two step process such as RMC in that the intermediate states have to be treated as elementary particles as well. Thus effects coming from the excitation of the intermediate nucleus, which are implicitly partially included in the IA, are not included in the EPM. A full investigation of this is beyond the scope of this paper, though see Ref. [18]. However one should keep this in mind as a caveat with respect to the EPM.

IV. THE IMPULSE APPROXIMATION

The impulse approximation method provides a simple ''microscopic'' picture of the nuclear reaction in terms of nucleons. In this picture, the constituent nucleons inside the nucleus are approximated as free (this is probably a good approximation as the binding energy of the trinucleon system is ~ 8 MeV, which is about 0.3% of the mass of the nucleus) and the nuclear reaction $^3\text{He}+\mu^-\rightarrow{}^3\text{H}+\nu_\mu+\gamma$ is viewed as the sum of its nucleon counterparts, $p+\mu^-\rightarrow n+\nu_\mu+\gamma$ (that is, only one-body currents are considered and two-body meson exchange currents are neglected or put in later as a correction). The extra degrees of freedom which arise from considering each nucleon of the nucleus instead of treating the nucleus as a whole are integrated out using realistic trinucleon wave functions. Given these assumptions, the whole problem boils down to separating the EPM and non-EPM degrees of freedom and finding the IA equivalent (denote it as M_{ia}) of $M(P_{^3\text{H}},P_{^3\text{He}},M_t)$ in the EPM. More explicitly, we want the $M(P_{^3\text{H}},P_{^3\text{He}},M_t)$ in Eq. (10) to be replaced with M_{ia} in order to find the IA version of $d\Gamma/dk$. The relationship between $M(P_{^3\text{H}},P_{^3\text{He}},M_t)$ and M_{ia} is

$$\begin{aligned}
&M(P_{^3\text{H}},P_{^3\text{He}},M_t)\\
&\quad\leftrightarrow \mathbf{3}\int\Bigg\{(2\pi)^3\delta^{(3)}(\vec{p}_\alpha{}'-\vec{p}_\alpha)(2\pi)^3\\
&\qquad\times\delta^{(3)}\left(\vec{q}_\alpha'-\vec{q}_\alpha+\frac{2}{3}(\vec{\nu}+\vec{k}-\vec{\mu})\right)\\
&\qquad\times\psi^*_{^3\text{H}}(\vec{p}_\alpha{}',\vec{q}_\alpha')\psi_{^3\text{He}}\ (\vec{p}_\alpha,\vec{q}_\alpha)\\
&\qquad\times M(k'_\alpha,k_\alpha,M_p)\frac{d^3\vec{q}_\alpha'}{(2\pi)^3}\frac{d^3\vec{p}_\alpha{}'}{(2\pi)^3}\frac{d^3\vec{q}_\alpha}{(2\pi)^3}\frac{d^3\vec{p}_\alpha}{(2\pi)^3}\Bigg\}\\
&\quad\equiv M_{ia},
\end{aligned}\tag{18}$$

where $k_\alpha,k_\beta,k_\gamma$ $(k'_\alpha,k'_\beta,k'_\gamma)$ denote the four-momenta of the three initial (final) nucleons α, β, and γ. The (three-) momentum transformation separating the EPM and non-EPM degrees of freedom is

$$\begin{aligned}
\vec{P}&=\vec{k}_\alpha+\vec{k}_\beta+\vec{k}_\gamma,\\
\vec{q}_\alpha&=\frac{2}{3}\vec{k}_\alpha-\frac{1}{3}\vec{k}_\beta-\frac{1}{3}\vec{k}_\gamma,\\
\vec{p}_\alpha&=\frac{1}{2}\vec{k}_\beta-\frac{1}{2}\vec{k}_\gamma
\end{aligned}\tag{19}$$

for the initial nucleus, with an identical transformation law for the final nucleus. It is obvious that $\vec{P}$ (a EPM degree of freedom) is the center of mass momentum vector of the nucleus and $\vec{q}_\alpha$ (a non-EPM degree of freedom) is the momentum of nucleon α (spectator) with respect to the center of mass momentum of the other two nucleons (subsystem) while $\vec{p}_\alpha$ (a non-EPM degree of freedom) is the momentum of particle β with respect to particle γ.[2] The **3** comes from the antisymmetrization of the wave function and it allows one to let the current operator act on a particular nucleon (chosen to be nucleon α) three times instead of acting on each nucleon of the nucleus.

The parametrization of the nucleon form factors is exactly the same as that of the nuclear ones [see Eq. (16)]. For convenience in notation, we change $F_i\rightarrow g_i$ and $R_i\rightarrow r_i$ in Eq. (16) to denote the nucleon case. The various parameters for nucleon form factors are $g_V(0)=1$, $r_V=0.7589$ fm [7], $g_M(0)=\kappa_p-\kappa_n$, $r_M=0.8781$ fm [7], $g_A(0)=-1.267\pm0.0035$ [19], $r_A=0.6580$ fm [7].

The momentum space trinucleon wave functions [20,21] are realistic wave functions derived from the Faddeev equation (see, for example, Ref. [22]) with different model potentials. Each one of them has 22 channels that contain all possible states up to and including $J=2$, where J is the total angular momentum of the subsystem particles. They can be written as

$$|\Psi\rangle=\sum_{i_c}\ \psi_{i_c}(p_\alpha,q_\alpha)|i_c\rangle|\vec{P}\rangle, \tag{20}$$

where i_c is the channel number and $|\vec{P}\rangle$ is the center of mass momentum of the trinucleon system, which we will not write explicitly from now on. The coupling scheme of the channels is

$$|i_c\rangle=|([L_\alpha l_\alpha]\mathcal{L}_\alpha,[S_\alpha s_\alpha]\mathcal{S}_\alpha)\mathcal{J}\rangle|(I_\alpha i_\alpha)\mathcal{I}\rangle\equiv|i_c(\mathcal{J})\rangle|i_c(\mathcal{I})\rangle. \tag{21}$$

The spin and angular momentum part is given by $|([L_\alpha l_\alpha]\mathcal{L}_\alpha,[S_\alpha s_\alpha]\mathcal{S}_\alpha)\mathcal{J}\rangle$ with L_α (S_α) the angular momentum (spin) of the subsystem $(\beta\gamma)$ and l_α (s_α) the angular momentum (spin) of particle α (the spectator particle). These are coupled to form $\mathcal{L}_\alpha$ $(\mathcal{S}_\alpha)$ and then to $\mathcal{J}=\frac{1}{2}$. The $|(I_\alpha i_\alpha)\mathcal{I}\rangle$ is the isospin, part, with I_α being the subsystem isospin which couples with i_α, the spectator isospin, to form $\mathcal{I}=\frac{1}{2}$.

[2] $\vec{p}_\alpha$ and $\vec{q}_\alpha$ will sometimes be denoted as $\vec{p}$ and $\vec{q}$ when no confusion arises.

It is now clear that $\psi_{^3\mathrm{He}}(\vec{p}_\alpha,\vec{q}_\alpha)$ in Eq. (18) is just the $\langle\hat{p},\hat{q}|$ projection of Eq. (20),

$$\psi_{^3\mathrm{He}}(\vec{p}_\alpha,\vec{q}_\alpha)=\sum_{i_c}\psi_{i_c}(p_\alpha,q_\alpha)\langle\hat{p},\hat{q}|i_c\rangle, \tag{22}$$

where

$$\langle\hat{p},\hat{q}|i_c\rangle=[Y^{\mathcal{L}}_{L\,l}(\hat{p},\hat{q})\otimes\chi^{\mathcal{S}}_{Ss}]^{M_{\mathcal{J}}}_{\mathcal{J}}\eta^{\mathcal{I}M_{\mathcal{I}}}_{Ii}. \tag{23}$$

Note that Eq. (26) below defines the bipolar harmonic $Y^{\mathcal{L}}_{L\,l}(\hat{p},\hat{q})$. χ and η in the above equation are spinors and isospinors, respectively. Their coupling method is exactly the same as the bipolar harmonic in Eq. (26).

To put M_{ia} in Eq. (18) into a useful format, we have to expand $M(k'_\alpha,k_\alpha,M_p)$ nonrelativistically in powers of the struck nucleon momentum $\vec{k}_\alpha$ (which equals $\vec{q}_\alpha$ upon setting the initial center of mass momentum of the trinucleon zero) and the δ functions into angular momentum eigenstates. Upon setting $\vec{\mu}=0$ and denoting $\vec{s}\equiv\vec{\nu}+\vec{k}$, the δ functions can be expanded as [see Ref. [23] for definitions of spherical Bessel functions $j_l(x)$]

$$(2\pi)^3\delta^{(3)}(\vec{p}'_\alpha-\vec{p}_\alpha)=(2\pi)^3\frac{\delta(p'_\alpha-p_\alpha)}{p^2_\alpha}\sum_l(-1)^l\sqrt{2l+1}Y^{0\,0}_{l\,l}(\hat{p}'_\alpha,\hat{p}_\alpha), \tag{24}$$

$$(2\pi)^3\delta^{(3)}\left(\vec{q}'_\alpha-\vec{q}_\alpha+\frac{2}{3}\vec{s}\right)=\sum_{\substack{l_i,m_3\\ i=1-3}}\sqrt{\frac{(4\pi)^5(2l_1+1)(2l_2+1)}{(2l_3+1)}}\times\begin{pmatrix}l_3 & l_1 & l_2\\ 0 & 0 & 0\end{pmatrix}i^{l_1-l_2+l_3}Y^{l_3-m_3}_{l_1l_2}(\hat{q}'_\alpha,\hat{q}_\alpha)Y^{-m_3}_{l_3}(\hat{s})^*\times\int j_{l_1}(q'_\alpha r)j_{l_2}(q_\alpha r)j_{l_3}\left(\frac{2}{3}sr\right)r^2dr, \tag{25}$$

$$Y^{l_3m_3}_{l_1l_2}(\hat{x},\hat{y})\equiv\sum_{m_1,m_2}\begin{pmatrix}l_3 & l_1 & l_2\\ m_3 & m_3-m_1 & m_2\end{pmatrix}Y^{m_1}_{l_1}(\hat{x})Y^{m_2}_{l_2}(\hat{y}). \tag{26}$$

The notations used here are the same as Brink and Satchler [24] except that the Clebsch-Gordon coefficients are denoted by

$$\begin{pmatrix}J & J_1 & J_2\\ M & M_1 & M_2\end{pmatrix}$$

as opposed to $\langle JM|J_1J_2M_1M_2\rangle$. The next thing after the expansion is to couple all the spin and angular momentum operators in Eq. (18) into tensors of rank 0 or 1. Since the total angular momentum of both initial and final states is $\frac{1}{2}$, there is no need to couple the operators into tensors of other ranks. There is also no need to couple operators into odd parity quantities as both the initial and final states are of even parity. Recognizing the total angular momentum of the trinucleon system in the IA as the spin in the EPM, one can easily see that any operators of rank 1 in the IA correspond to (within a factor) $\vec{\sigma}$ matrices in the EPM, and operators of rank 0 in the IA correspond to identity hadronic operators in the EPM.

All the coefficients in $M(k'_\alpha,k_\alpha,M_p)$ are expanded to $O(\vec{q}/M_p)$ except that of g_P. The kinematic end points of RMC are quite close to the poles of g_P and thus might make its value large at those places. Therefore, coefficients of g_P are expanded to $O([\vec{q}/M_p]^2)$.

The correspondence between the IA and the EPM for all forms of operators up to first order in momentum is shown below. Operators of higher order in momentum will not be shown owing to the lack of space. Note that the $[\cdots]$'s are actually reduced matrix elements between the initial and final states (i.e., results of integration of ''internal'' degrees of freedom) and the numbers inside denote some specific spin and angular momentum combination. They will be defined in Eq. (33). For now, it is sufficient to note that the first digit of $[\cdots]$ is related to the nucleon momentum $\vec{q}$ (for example, 0 indicates no nucleon momentum, 1 indicates $\vec{q}$) and the second digit comes from the spherical harmonics of the δ function. These two terms couple together to an angular momentum value represented by the third digit. The fourth digit is related to the hadronic spin matrix and the subscript is the rank of the whole reduced matrix element. **1** (or sometimes denoted as $\mathbf{1}_0$) is defined as the hadronic identity matrix element in both the IA and the EPM. It differs from $[\mathbf{1}]^0$ (see Ref. [25]), although they are related.

The IA expressions, after coupling and reexpressing in EPM format, become

$$\mathbf{1}\leftrightarrow[\{(0,0)0\otimes0\}_0]\mathbf{1}, \tag{27}$$

$$\vec{\sigma}\cdot\vec{v}\leftrightarrow-\frac{3}{\sqrt{2}}[\{(0,2)2\otimes1\}_1]\vec{\sigma}\cdot\hat{s}\vec{v}\cdot\hat{s}+\left\{\frac{1}{\sqrt{2}}[\{(0,2)2\otimes1\}_1]+[\{(0,0)0\otimes1\}_1]\right\}\vec{\sigma}\cdot\vec{v}, \tag{28}$$

$$\vec{\sigma}\cdot\vec{q}\leftrightarrow\left\{-\sqrt{\frac{5}{3}}[\{(1,1)2\otimes1\}_1]-\frac{1}{2}[\{(1,1)1\otimes1\}_1]-\frac{1}{\sqrt{3}}[\{(1,1)0\otimes1\}_1]\right\}\vec{\sigma}\cdot\hat{s}, \tag{29}$$

$$\vec{q}\cdot\vec{v}\leftrightarrow-\frac{1}{\sqrt{3}}[\{(1,1)0\otimes0\}_0]\vec{v}\cdot\hat{s}-\frac{i}{\sqrt{2}}[\{(1,1)1\otimes0\}_1]\vec{\sigma}\cdot\vec{v}\times\hat{s}, \tag{30}$$

$$\vec{\sigma}\times\vec{q}\cdot\vec{v}\leftrightarrow\left\{-\sqrt{\frac{5}{12}}[\{(1,1)2\otimes 1\}_1]+\frac{1}{2}[\{(1,1)1\otimes 1\}_1]+\sqrt{\frac{1}{3}}[\{(1,1)0\otimes 1\}_1]\right\}\vec{v}\times\hat{s}\cdot\vec{\sigma}+i\sqrt{\frac{2}{3}}[\{(1,1)1\otimes 1\}_0]\vec{v}\cdot\hat{s}, \tag{31}$$

$$\begin{aligned}\vec{q}\cdot\vec{v}\vec{\sigma}\cdot\vec{u}\leftrightarrow&\left\{\sqrt{\frac{1}{15}}[\{(1,1)2\otimes 1\}_1]-\sqrt{\frac{1}{3}}[\{(1,1)0\otimes 1\}_1]-\frac{1}{2}\sqrt{\frac{2}{5}}[\{(1,3)2\otimes 1\}_1]\right\}\vec{\sigma}\cdot\vec{u}\vec{v}\cdot\hat{s}\\&+\left\{-\sqrt{\frac{3}{20}}[\{(1,1)2\otimes 1\}_1]+\frac{1}{2}[\{(1,1)1\otimes 1\}_1]-\frac{1}{2}\sqrt{\frac{2}{5}}[\{(1,3)2\otimes 1\}_1]\right\}\vec{\sigma}\cdot\vec{v}\vec{u}\cdot\hat{s}\\&+\left\{-\sqrt{\frac{3}{20}}[\{(1,1)2\otimes 1\}_1]-\frac{1}{2}[\{(1,1)1\otimes 1\}_1]-\frac{1}{2}\sqrt{\frac{2}{5}}[\{(1,3)2\otimes 1\}_1]\right\}\vec{\sigma}\cdot\hat{s}\vec{u}\cdot\vec{v}\\&+\sqrt{\frac{5}{2}}[\{(1,3)2\otimes 1\}_1]\vec{\sigma}\cdot\hat{s}\vec{u}\cdot\hat{s}\vec{v}\cdot\hat{s}+i\sqrt{\frac{1}{6}}[\{(1,1)1\otimes 1\}_0]\vec{u}\cdot\vec{v}\times\hat{s}.\end{aligned} \tag{32}$$

Note that while $\vec{\sigma}$ on the left hand side acts on the spin of the spectator nucleon, $\vec{\sigma}$ on the right acts on the entire *nucleus* and that $\vec{u}$ and $\vec{v}$ are mutually commuting vectors that are *not* concerned with the internal momenta (i.e. not $\vec{p}$ nor $\vec{q}$) and commute with $\vec{\sigma}$. Using Delorme's [25] notation, $[\mathbf{1}]^0=[\{(0,0)0\otimes 0\}_0]$, $[\vec{\sigma}]^{0,1}=[\{(0,0)0\otimes 1\}_1]$, $[\vec{\sigma}]^{2,1}=-[\{(0,2)2\otimes 1\}_1]$, $[\vec{\sigma}]^{+}=[\vec{\sigma}]^{0,1}+\sqrt{2}[\vec{\sigma}]^{2,1}$, and $[\vec{\sigma}]^{-}=[\vec{\sigma}]^{0,1}-(1/\sqrt{2})[\vec{\sigma}]^{2,1}$. The precise relationship between $[i\vec{P}]^{1,1}$ and the reduced matrix elements defined here is unclear, but has a magnitude of the order of $[\{(1,1)1\otimes 0\}_1]$ or $[\{(1,1)1\otimes 1\}_1]$. As one will see later, these two matrix elements are very small.

The definition of $[\{(a,b)c[\bar{a}]\otimes d\}_e]$ (a function of $s\equiv\|\vec{\nu}+\vec{k}\|$) is

$$\begin{aligned}[\{(a,b)c[\bar{a}]\otimes d\}_e]\equiv&\mathbf{3}\frac{1}{2\pi^5}\left\langle\frac{1}{2}\middle\|T_e\middle\|\frac{1}{2}\right\rangle^{-1}\left\langle\frac{1}{2}\middle\|\vec{\tau}\middle\|\frac{1}{2}\right\rangle^{-1}\sum_{i_c,i_c'}\sum_{l_1,l_2,L_1}(-1)^{L_1-l_1-l_2+b}\int\left\{p^2dp\,r^2dr j_b\left(\frac{2}{3}sr\right)\right.\\&\left.\times\{\psi^*_{i_c'}(p,q')j_{l'}(q'r)q'^2dq'\}\{\psi_{i_c}(p,q)j_{l_2}(qr)q^{2+\bar{a}}dq\}\right\}\begin{pmatrix}b & l_1 & l_2\\ 0 & 0 & 0\end{pmatrix}\\&\times F(l_1,l_2;a,b,c;i_c',i_c)\sqrt{\frac{(2L_1+1)(2l_2+1)(2l_1+1)}{2b+1}}\\&\times\langle i_c'(\mathcal{J})\|\{[Y^0_{L_1,L_1}(\hat{p}',\hat{p})\otimes Y^c_{l',l}(\hat{q}',\hat{q})]\otimes(\mathbf{1}_0\otimes T_d)\}_e\|i_c(\mathcal{J})\rangle\langle i_c'(\mathcal{I})\|(\mathbf{1}_0\otimes\vec{\tau})\|i_c(\mathcal{I})\rangle,\end{aligned} \tag{33}$$

TABLE I. Various OMC and RMC statistical rates calculated with g_P or F_P at the PCAC value. The numbers in the second column are the values obtained by using the "$\vec{\nu}/3$" prescription up to $\mathcal{O}(\vec{q}/M_p)$ terms. The numbers in the third column are obtained via the correct approach up to $\mathcal{O}(\vec{q}/M_p)$ terms. The fourth column has values of the OMC rates using "$\vec{\nu}/3$" prescription up to $\mathcal{O}([\vec{q}/M_p]^2)$ terms. Numbers in the fifth column are the values obtained by the correct approach up to $\mathcal{O}([\vec{q}/M_p]^2)$ terms; the sixth and rightmost columns contain $\Gamma^{RMC}_{stat}(k>5$ MeV) and $\Gamma^{RMC}_{stat}(k>57$ MeV), respectively. CD Bonn stands for charge dependent Bonn and AV14 for Argonne V14 potentials.

Potentials	OMC rate (statistical) (s^{-1})				Γ^{RMC}_{stat} (s^{-1})	
	$\mathcal{O}\left(\frac{\vec{q}}{M_p}\right)$; $\frac{\vec{\nu}}{3}$	$\mathcal{O}\left(\frac{\vec{q}}{M_p}\right)$; full	$\mathcal{O}\left(\frac{\vec{q}^2}{M_p^2}\right)$; $\frac{\vec{\nu}}{3}$	$\mathcal{O}\left(\frac{\vec{q}^2}{M_p^2}\right)$; full	$k>5$ MeV	$k>57$ MeV
Bonn *A*	1368.6	1368.1	1367.8	1357.9	0.6255	0.1691
Bonn *B*	1341.3	1340.8	1340.4	1330.7	0.6164	0.1666
CD Bonn	1336.1	1335.7	1335.3	1326.1	0.6153	0.1663
Nijmegen I	1298.0	1297.5	1297.1	1288.2	0.6023	0.1626
Paris	1270.9	1270.4	1270.1	1260.3	0.5932	0.1602
AV14	1271.0	1270.6	1270.2	1260.0	0.5929	0.1601
EPM		1503			0.8263	0.2451

where $T_{d(e)}=\mathbf{1}_0$ for $d(e)=0$ and $\vec{\sigma}$ for $d(e)=1$; $\vec{\tau}$ is the isospin operator. Notice $\overline{a}$ specifies the (mass) dimension of the matrix element. When $\overline{a}$ is not shown explicitly on a reduced matrix element, $\overline{a}=a$; that is, $[\{(a,b)c\otimes d\}_e] \equiv[\{(a,b)c[a]\otimes d\}_e]$. $F(l_1,l_2;a,b,c;i_c',i_c)$ is defined as

$$F(l_1,l_2;a,b,c;i_c',i_c)\equiv\begin{pmatrix} c & a & b \\ m_c & m_a & m_b \end{pmatrix}^{-1}\int Y_{l',l}^{c,m_c}(\hat{v},\hat{\chi})^* Y_{0,a}^{a,m_a}(\hat{v},\hat{\chi}) Y_{l_1,l_2}^{b,m_b}(\hat{v},\hat{\chi}) d\hat{v} d\hat{\chi}$$

$$=\frac{1}{4\pi}(-1)^{l_1+l_2+b}\begin{Bmatrix} l_1 & l_2 & b \\ a & c & l \end{Bmatrix}\begin{pmatrix} l & l_2 & a \\ 0 & 0 & 0 \end{pmatrix}\sqrt{\frac{(2l_2+1)(2a+1)}{2b+1}}\delta_{l_1 l'}, \tag{34}$$

$\hat{v},\hat{\chi}$ being some dummy angular variables.

$\langle i_c'(\mathcal{J})\|([Y^0_{L_1,L_1}(\hat{p}',\hat{p})\otimes Y^c_{l',l}(\hat{q}',\hat{q})]\otimes(\mathbf{1}_0\otimes T_d))_e\|i_c(\mathcal{J})$ is the spin and angular momentum part of the reduced matrix element between the helion and triton channels. Its calculation is tedious but standard.

$$\langle i_c'(\mathcal{J})\|([Y^0_{L_1,L_1}(\hat{p}',\hat{p})\otimes Y^c_{l',l}(\hat{q}',\hat{q})]\otimes(\mathbf{1}_0\otimes T_d))_e\|i_c(\mathcal{J})\rangle$$

$$=4\pi(-1)^{\mathcal{L}'+2l+c+L'+\mathcal{S}'+\frac{1}{2}+S'+d}\{(2\mathcal{L}+1)(2\mathcal{L}'+1)$$

$$\times(2\mathcal{S}+1)(2\mathcal{S}'+1)(2c+1)(2e+1)\}^{1/2}$$

$$\times\begin{Bmatrix} \frac{1}{2} & \frac{1}{2} & e \\ \mathcal{L}' & \mathcal{L} & c \\ \mathcal{S}' & \mathcal{S} & d \end{Bmatrix}\begin{Bmatrix} \mathcal{L} & \mathcal{L}' & c \\ l' & l & L' \end{Bmatrix}\begin{Bmatrix} \mathcal{S} & \mathcal{S}' & d \\ \frac{1}{2} & \frac{1}{2} & S' \end{Bmatrix}$$

$$\times\delta_{SS'}\left\langle\frac{1}{2}\middle\|T_d\middle\|\frac{1}{2}\right\rangle\langle L' \ 0\|Y^0_{L_1,L_1}(\hat{p}',\hat{p})\|0 \ L\rangle. \tag{35}$$

Note also that

$$\sum_{L_1}(-1)^{L_1}\sqrt{2L_1+1}\langle L' \ 0\|Y^0_{L_1,L_1}(\hat{p}',\hat{p})\|0 \ L\rangle=\frac{1}{4\pi}\delta_{LL'}. \tag{36}$$

$\langle i_c'(\mathcal{I})\|\mathbf{1}_0\otimes\vec{\tau}\|i_c(\mathcal{I})\rangle$ is the isospin contribution of the reduced matrix element, which equals

$$2(-1)^{I'}\begin{Bmatrix} 1/2 & 1/2 & 1/2 \\ 1/2 & 1/2 & I' \end{Bmatrix}\delta_{II'}\left\langle\frac{1}{2}\middle\|\vec{\tau}\middle\|\frac{1}{2}\right\rangle. \tag{37}$$

By following through all the procedures mentioned in this section, it is possible to match the IA amplitude piece by piece with its EPM counterparts and thus make a direct comparison between each piece. In other words, we have arranged the nonzero terms of M_{ia} to depend only on the EPM degrees of freedom. We then obtain $d\Gamma/dk$ via Eq. (10) with $M(P_{^3\mathrm{H}},P_{^3\mathrm{He}},M_t)$ replaced by M_{ia}.

V. RESULTS AND DISCUSSION

A. Results

We have calculated the rate for OMC, and the photon spectrum and integrated rate for RMC, in both IA and EPM approaches, using the formalism described in the preceding sections. Table I shows various RMC and OMC statistical rates, with the final results given in the last three columns. Figure 3 shows the IA RMC spectra for various wave functions together with the EPM spectrum.

One sees immediately that the IA results are significantly lower than the EPM results both for OMC and RMC. This is consistent with the OMC results of Refs. [7,8]. For OMC the

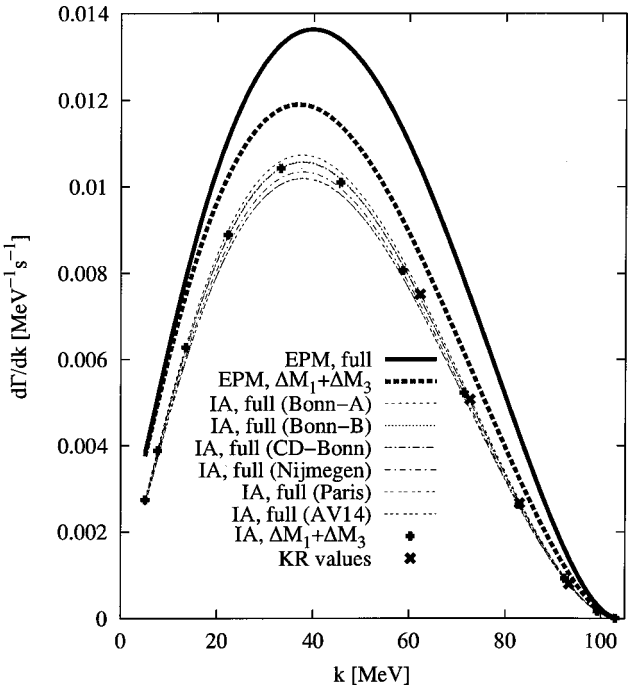

FIG. 3. RMC photon spectra from two EPM calculations, one with the full Adler and Dothan amplitude ΔM and the other with only the terms $\Delta M_1+\Delta M_3$ necessary for gauge invariance. Also included are RMC photon spectra from the full IA calculation using various model potentials, along with one example with only $\Delta M_1+\Delta M_3$. All wave functions used have 22 Faddeev components and the permutation is projected on the same set of states. The infrared divergent part is not shown. The KR values come from Klieb and Rood [5,6] and are their IA calculation results.

difference is understood to arise from various meson exchange corrections, which are included implicitly in the EPM approach but which must be put into the IA by hand as specific corrections. [9]. Presumably a similar explanation holds for RMC.

B. Importance of various ingredients

We can see from these results the importance of some of the specific ingredients and improvements that we have included in the calculations. In particular, Table I shows the results obtained for the IA statistical OMC rate using four different methods of treating the nucleon momentum operator $\vec{q}$. The most common way of treating this operator is to replace $\vec{q}$ with $\vec{\nu}/3$ [26] (second column) and virtually all existing OMC calculations used this method. However, this method is strictly correct only for S waves to first order in nucleon momentum. Using the correct approach discussed in Sec. IV and keeping terms up to $O(\vec{q}/M_p)$ decreases the OMC statistical rate by about 0.5 s^{-1} (third column) as compared to the results from the $\vec{\nu}/3$ prescription. The smallness of the effect is primarily due to the minute contribution of the P-state wave function to the trinucleon wave function.[3] There is a difference of about 10 s^{-1} between using the $\vec{\nu}/3$ approach (fourth column) and the correct approach (fifth column) when terms up to $O(\vec{q}^2/M_p^2)$ are kept. Although in percentage terms it is just about 0.6%, it is much larger than the 0.5 s^{-1} difference between the numbers in the second and third columns. This is perhaps to be expected as the $\vec{\nu}/3$ approach cannot be applied to terms higher than first order in nucleon momentum.

Table I and Fig. 3 also show the dependence of both the IA OMC and RMC calculations on various trinucleon potentials. In general, the Bonn-type potentials seem to give higher (and perhaps better) RMC and OMC results than the other potentials. To analyze this properly, let us take a look at the three dominant reduced matrix elements, $[\mathbf{1}]^0$, $[\vec{\sigma}]^{0,1}$, and $[\vec{\sigma}]^{2,1}$, which are shown as a function of s in Figs. 4–6. All the curves produced by non-Bonn potentials seem to be a bit separated from the curves of the Bonn-type potentials, especially in the region where s is large. For $[\mathbf{1}]^0$ the problem may be partly associated with the numerical normalization since $[\mathbf{1}]^0$ $(s=0)$ should be unity, in principle. However, even though one takes this into account (say, for example, by scaling the curves so that they agree with each other at $s=0$) the values of $[\mathbf{1}]^0$ for the non-Bonn potentials are still smaller than that of the Bonn potentials, as can be easily seen from the fact that the fractional deviation of the reduced matrix element among various wave functions is larger at large values of s.

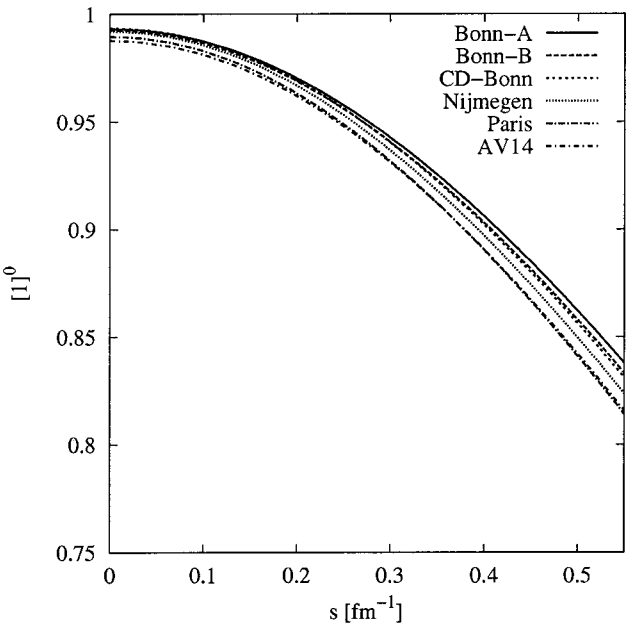

FIG. 4. Plot of $[\mathbf{1}]^0$ vs s for different nuclear potentials.

This seems to have something to do with the different binding energies produced by the Bonn and non-Bonn potentials. The non-Bonn potentials generally underbind the trinucleon by about 0.5 to 1 MeV. Congleton and Truhlik [9] pointed out that[4] $[\mathbf{1}]^0 \sim 1 - \text{const} \times \langle r^2 \rangle s^2$ and that $\langle r^2 \rangle$ scales like the inverse of the binding energy, and thus argued that one can expect a lower value for $[\mathbf{1}]^0$ when a wave function with a lower binding energy is used.[5] For $[\vec{\sigma}]^{0,1}$, they further argued that since it is a reduced matrix element for one-body currents (this IA calculation contains only one-body currents), the Bonn potential's weak tensor force makes this matrix element large in magnitude. If their analysis is correct, this would potentially explain why the Bonn-type potentials consistently give higher results in both OMC and RMC IA calculations. The quadraticlike curve of $[\vec{\sigma}]^{2,1}$ is obvious if one notices $j_2(x) \sim x^2/15$ for $x \ll 1$. Since $[\vec{\sigma}]^{2,1}$ is the result of S-D overlap, a trinucleon wave function with a larger component of D wave would probably have a larger magnitude of $[\vec{\sigma}]^{2,1}$, which seems to be the case for the generally higher D-wave components of the non-Bonn potentials (see Appendix (B)).

Recently Lahiff and Afnan [27] suggested that the Bonn-type potentials might be a better choice than the Nijmegen potential because the energy dependence of propagators is treated exactly (during the evaluation of the potential via

[3]Note that this effect is a *genuine* effect and not an effect caused by numerical calculation. To prove this, a two channel Yamaguchi wave function consisting solely of S waves is used to gauge the numerical uncertainty in wave function integration. There is an *increase* of the rate (due only to numerical integration) by 0.1 s^{-1}, out of a total 1600 s^{-1}, for the correct approach. This difference is much smaller than the difference (stemming from errors in *both* the numerical integration and the $\vec{\nu}/3$ approach) of the calculations of the other regular 22-channel wave functions.

[4]To see this, expand $j_0(\frac{2}{3}sr)$ in polynomials and note that const>0.

[5]To define the term ''lower binding energy,'' note that Appendix B shows that the Bonn potentials have the highest binding energy predictions among all the wave functions.

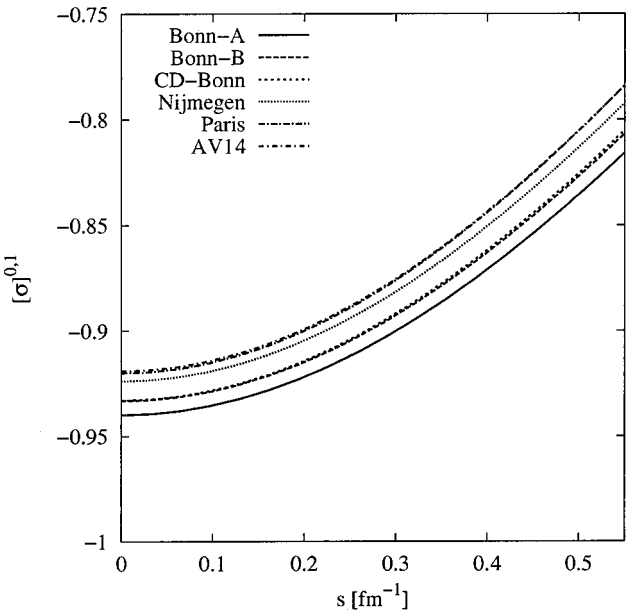

FIG. 5. Plot of $[\vec{\sigma}]^{0,1}$ vs s.

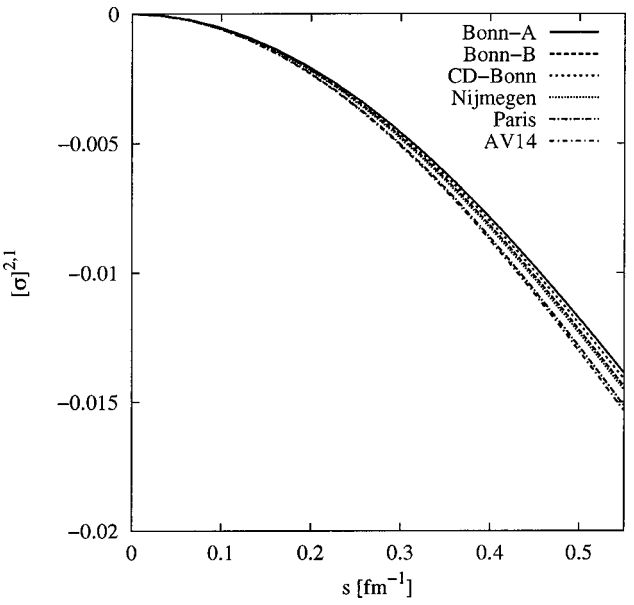

FIG. 6. Plot of $[\vec{\sigma}]^{2,1}$ vs s.

time-ordered perturbation theory) in the Bonn-type potential, but the Nijmegen group removes this energy dependence.

Thus to summarize, the reason that the Bonn-type potentials give a higher result for both RMC and OMC may primarily be due to its higher binding energy and possibly its weak tensor force. The higher D-wave components of those non-Bonn potentials may give a boost to $[\vec{\sigma}]^{2,1}$ but the smallness of $[\vec{\sigma}]^{2,1}$ as compared to the other two would make its effect on the IA capture rates small.

The effects of the Adler and Dothan terms can also be seen in Fig. 3. The upper two curves show the RMC spectrum including the full ΔM of Eq. (5) and including only $\Delta M_1+\Delta M_3$, the part required by GI. There is clearly a significant difference between these two photon spectra in the EPM. The photon spectrum with the full Adler and Dothan amplitude is 5–25 % higher for photon momentum starting from 20 MeV than the one with terms only to ensure GI.

The figure also shows six IA photon spectra for different trinucleon wave functions using the full set of Adler and Dothan terms plus an IA photon spectrum with just terms of $\Delta M_1+\Delta M_3$ necessary to ensure GI. For this latter case a trinucleon wave function from the Bonn-A potential was used for the calculation. For the IA case there is almost no observable change in the photon spectrum produced by including the full set of Adler-Dothan terms as opposed to just those required for GI.

If one considers IA and EPM spectra with only the terms from $\Delta M_1+\Delta M_3$, i.e., only those necessary to ensure GI, the ratio of IA to EPM RMC total capture rate is similar to that of the corresponding OMC quantity ($\sim$83–90 %). However, as a result of the increased importance of the full set of Adler and Dothan terms in the EPM case, once these additional terms are included, the IA to EPM RMC capture rate ratio drops by more than 10% to around 73%.

An obvious reason for this increased sensitivity in the EPM case might be the more rapidly varying form factors in the nuclear case as opposed to the nucleon case. However there is also a relative sign flip between $F_A(0)$ and $g_A(0)$, which might play a role. To investigate this further we have done three things. We have artificially increased r_V, r_M, and r_A to 1.95 fm (a value comparable to various nuclear radii) and calculated the resulting IA photon spectra using these values (Fig. 7). We have calculated another set of photon spectra by flipping the sign of g_A in the IA (Fig. 8). We also provide the IA photon spectra when *both* of these effects are present (Fig. 9).

By looking at Figs. 7–9, one concludes that the IA RMC calculation would have shown a sensitivity to the additional terms in the full ΔM if the nucleon radii were of a size

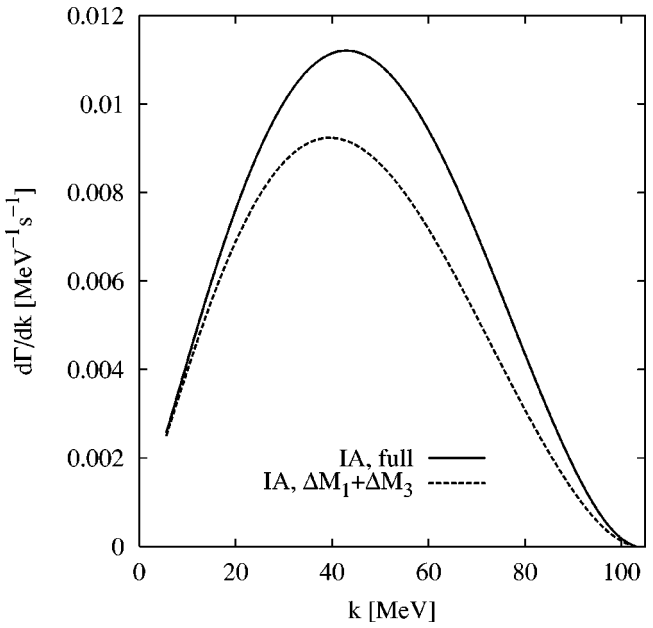

FIG. 7. Effect of increased nucleon radii on the full IA photon spectrum and on the spectrum with only $\Delta M_1+\Delta M_3$.

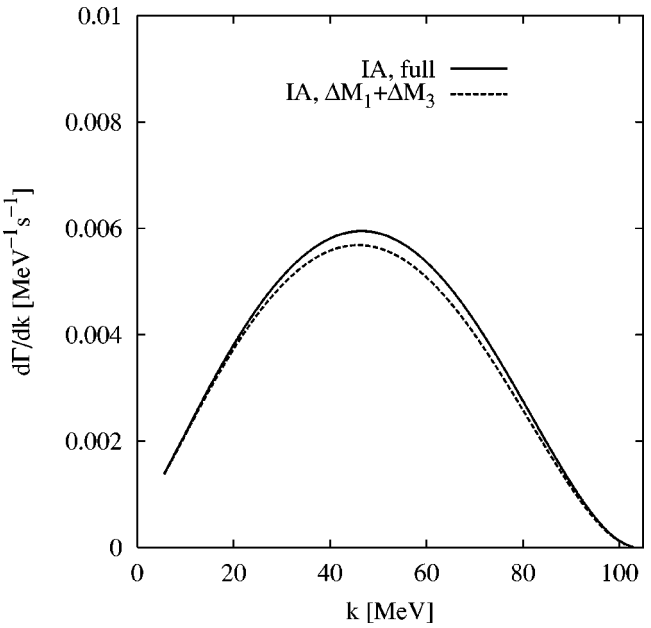

FIG. 8. Effect of changing the sign of g_A on the two sets of IA photon spectrum.

comparable to the nuclear ones, regardless of whether the sign of g_A is flipped (as in Fig. 9) or not (as in Fig. 7). The flipping of the sign of g_A decreases both spectra (full IA and calculation with only terms to ensure GI), but the difference between them is relatively small, provided the various nucleon radii are not artificially increased (Fig. 8).

One notes that there are some additional deficiencies of the Adler and Dothan procedure that may be relevant. In particular, $\mathcal{O}(kQ)$ terms in ΔM, which are formally of the same size as some terms that are kept, cannot be determined uniquely by GI or CVC and PCAC alone. As a result, some

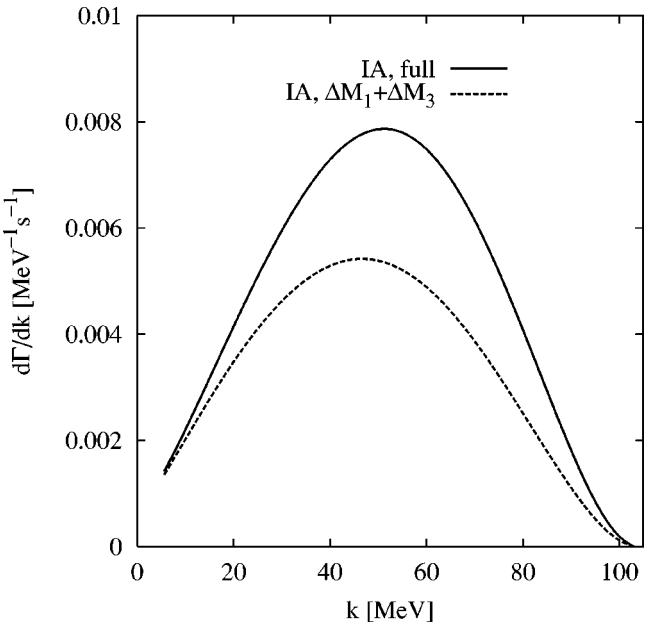

FIG. 9. Two sets of IA photon spectrum using *both* the increased nucleon radii *and* the sign change for g_A.

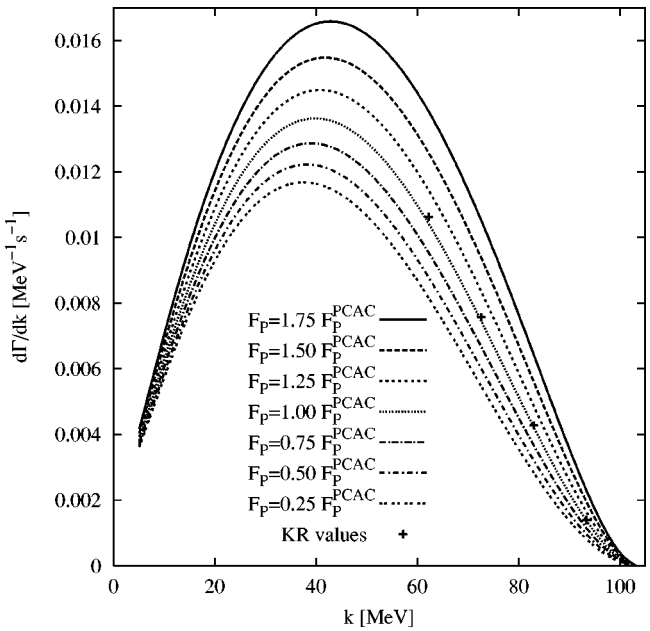

FIG. 10. The RMC photon spectrum $d\Gamma_{stat}/dk$ calculated in the EPM approach using the full Adler-Dothan amplitude with various values of F_P, in units of F_P^{PCAC} as determined from Eq. (4) with $\varepsilon=0$. The KR values are those of Klieb and Rood, taken from the relativistic calculation of Ref. [6], which are not shown in Ref. [5]

terms in ΔM involving derivatives of form factors are missing. This might be problematic when those derivatives are large, as in the EPM.

A final remark should be made regarding the comparison of the IA and EPM approaches. A major difference probably originates in the fact that the IA as described here uses only one-body currents. To elucidate this difference one needs to perform a more detailed investigation of the interactions of the nucleons using a model, say, involving meson exchanges and adding two- (or more-) body currents. These steps would entail a much more complicated calculation than that here, which considers only one-body currents. Congleton and Truhlik [9] calculated the meson exchange current (MEC) contribution to the simpler problem of OMC by ^{3}He and found that the IA+MEC prediction of the exclusive OMC statistical rate agrees with both the EPM calculation and experiment [28].[6] Clearly something similar needs to be done for RMC. Finally one should note that there are also difficulties with the EPM as applied to RMC relating to the treatment of intermediate nuclear states, as was discussed in Ref. [18].

C. Dependence on F_P

One of the main motivations for examining RMC is to obtain information about the induced pseudoscalar coupling constant and hence we have obtained results for various values of this coupling. Figure 10 shows the EPM calculation of the RMC photon spectrum for several different choices of F_P. There is an increase in the total capture rate and a slight

[6]They used a trinucleon wave function [29] that was derived in a slightly different way than those we use.

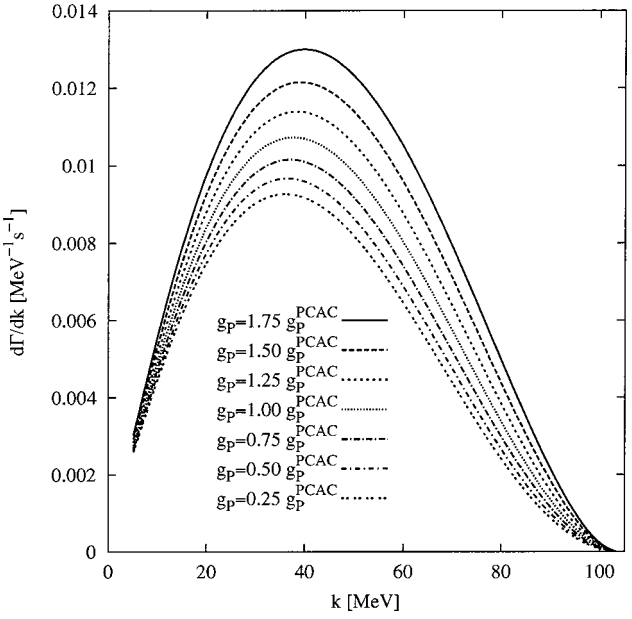

FIG. 11. Photon spectra from IA calculations for various values of g_P, in units of g_P^{PCAC}, as determined from Eq. (4) with $\varepsilon=0$. Wave functions derived from Bonn-*A* potential are used for the calculation.

shift of the peak of the spectrum to higher photon energy as one increases F_P from 0.25 to 1.75 times its PCAC value.

Figure 11 shows the same quantity as in Fig. 10 but for the IA calculation using wave functions derived from the Bonn-*A* potential. The qualitative features are essentially the same as for the EPM case, though the absolute magnitude is different, as was discussed above.

Figure 12 shows the sensitivity of the integrated spectrum, i.e., the RMC capture rate ($k>57$ MeV) with respect to the variation of F_P (for the EPM) and g_P (for the IA). The increase in the total capture rate as F_P or g_P increases from 0.25 to 1.75 times its PCAC value is slightly more rapid in the EPM than in the IA.

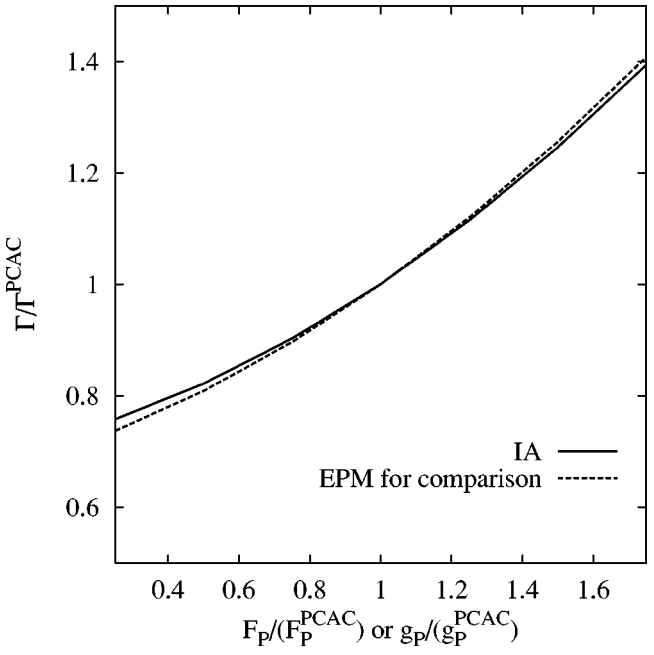

FIG. 12. Sensitivity of Γ_{stat}^{RMC} ($k>57$ MeV) to F_P or g_P. The Bonn-*A* potential was used for the IA calculations and the full ΔM was included for both IA and EPM results.

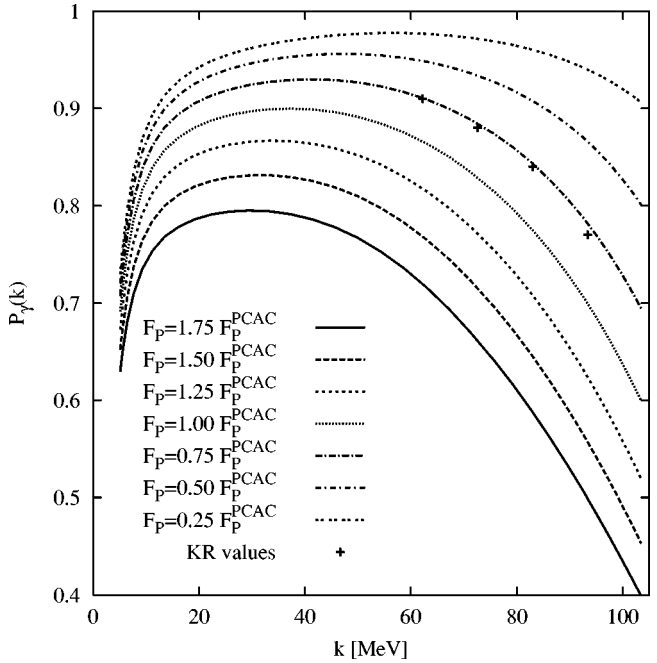

FIG. 13. Photon polarization for various values of F_P.

Another quantity which is sensitive to F_P in RMC and can, in principle, be considered, though the experiment is difficult, is the photon polarization. This is defined as the rate (or spectrum) for particular photon polarization minus that for the reversed polarization divided by the sum. Figure 13 shows this photon polarization $P_\gamma(k)$ using the EPM for various values of F_P. Clearly there is a very strong dependence on F_P, particularly for the highest energy photons. These photon polarizations for different values of F_P all seem to converge to a limit as $k\to 0$. This is due to the fact that in this limit the amplitude is determined by soft photon theorems. In the usual transverse gauge and for the initial muon and nucleus at rest, the leading term in the squared amplitude is $\mathcal{O}(1/k^2)$ and has the form $|\vec{P}_f\cdot\vec{\epsilon}_\lambda/M_n k|^2$ (from the diagram with the final hadron emitting). It is thus independent of the sign of the photon polarization, which makes $P_\gamma(k)\to 0$ as $k\to 0$.

Note that, although we have not calculated it explicitly, similar sensitivities to F_P would be expected in the photon asymmetry relative to the muon spin [30].

D. Comparison with other works

The EPM photon spectrum (Fig. 10) and total RMC rate, given in Table I, are in good agreement with the results of Klieb and Rood [5,6], who obtained a total rate of 0.814 s^{-1} [6] via a nonrelativistically approximated amplitude. Thus the extra terms included here but not included by Klieb and Rood seem not to contribute significantly to the photon spectrum. The agreement of the EPM OMC rate of 1503 s^{-1}

with Congleton and Fearing's [8] is also good, though this agreement is perhaps not surprising given that the values of the form factors used here, and the basic approach, are almost the same as theirs.

The IA calculation of the OMC rate using wave functions derived from Paris or AV14 potentials agrees with these of Klieb and Rood. However, the two IA RMC spectra are about 4% lower[7] than theirs. At first it looks a bit contradictory that more or less the same IA OMC rates, but slightly lower RMC results, are obtained in this work, but a closer look reveals that Klieb and Rood used a lot of approximations for evaluating the reduced matrix elements for the RMC spectrum, which they did not use for OMC.

In particular, instead of evaluating the reduced matrix elements directly in terms of s, they expressed $\hat{s}$ in terms of an infinite sum of spherical harmonics of $\hat{\nu}$ and $\hat{k}$ and imposed an artificial cutoff on this expansion. They also did not fully square the resulting matrix element. Only products of any two of the most dominant terms and products of one dominant and one small term were considered. In expanding the plane wave $\exp(i\vec{s}\cdot\vec{r})$, they only included the term having $j_0(\nu r)j_0(kr)$ and they used this approximation as the premise in deriving several relationships between various reduced matrix elements for RMC. They also do not seem to have expanded the spinor normalization factors $\sqrt{(M_p+k'^0_\alpha)/2k'^0_\alpha}$ (for the neutron spinor) and $\sqrt{(M_p+k^0_\alpha)/2k^0_\alpha}$ (for the proton spinor) quite consistently. None of these approximations were used here. Also some terms in ΔM that are present here but not included by Klieb and Rood tend to decrease the resulting photon spectrum a bit. Given these differences, the agreement within 4% for the rates is quite satisfactory.

The EPM photon polarization $P_\gamma(k)$ obtained in this work does differ from that of Klieb and Rood quite significantly (see Fig. 13). The reason behind this is that while the nonrelativistically reduced amplitude used by Klieb and Rood produces the correct spectrum within a few percent, it cannot produce $P_\gamma(k)$ accurately. Fearing [30] noted that the first order contribution to $P_\gamma(k)$ actually comes from $O(1/M_t^2)$ terms in the squared Hamiltonian. Klieb and Rood apparently compromised $P_\gamma(k)$'s accuracy by truncating many $\mathcal{O}(1/M_t^2)$ terms when they squared their already nonrelativistically reduced amplitude.

VI. SUMMARY AND CONCLUSION

We have performed a theoretical calculation of the process $^3\mathrm{He}+\mu^-\rightarrow{}^3\mathrm{H}+\gamma+\nu_\mu$ using two separate approaches, the elementary particle model and the impulse approximation. Our calculation contains a number of improvements over the previous ones, namely, (1) the full Adler and Dothan amplitude is used for both the EPM and IA calculations, (2) better momentum space wave functions from various nuclear potentials are employed for the IA calculation, (3) the nonrelativistic reduction of the IA amplitude contains second order nucleon momentum terms for coefficients of g_P, (4) the nucleon momentum terms in the IA are treated exactly without using the common $\vec{s}/3$ approach.

In general, our results agree well, when comparisons can be made, with the older calculations of Klieb and Rood [5,6]. In particular, using the EPM model approach, the RMC statistical rate obtained in this work agrees with that of Klieb and Rood. The photon polarization $P_\gamma(k)$ disagrees significantly with their results, which probably is a consequence of the fact that they truncated a lot of $\mathcal{O}(1/M_t^2)$ terms in the squared amplitude, which contribute significantly to $P_\gamma(k)$. The IA OMC results derived from wave functions of the non-Bonn potentials roughly agree with Klieb and Rood's but the RMC photon spectra from the same wave functions are slightly lower than Klieb and Rood's. This seems to have to do with the fact that they made some IA RMC specific approximations in evaluating their photon spectrum.

We summarize our results as follows. As expected there is a strong dependence of the results on the value of the induced pseudoscalar coupling constant F_P or g_P. There is a slight dependence of the IA calculations on nuclear potentials. The dependence can possibly be accounted for by the difference in the three-body binding energy resulting from the different potentials, by details of the nuclear potentials such as stronger/weaker tensor force, etc., and by differing partial wave characteristics of the resulting trinucleon wave functions.

There is quite a significant difference between the EPM and IA RMC calculations. A first look at the spectra would suggest that the difference is caused by the fact that the EPM calculation is much more sensitive than the IA to the $\mathcal{O}(k,k^2)$ terms in ΔM, which are larger in the EPM because of the much larger magnitude of the various nuclear radii than their nucleon counterparts. This hints at a poor convergence of these Adler and Dothan terms in the EPM and suggests that the higher order pieces, which cannot be calculated via the Adler-Dothan procedure, might be important. Further problems with the EPM have been discussed before in Ref. [18]. Probably the most important effect contributing to this difference, however, is the meson exchange corrections. These accounted for the difference between IA and EPM in the OMC case [9]. Such a calculation will be much more complicated for RMC, but is clearly needed to fully understand the differences between the IA and EPM approaches.

ACKNOWLEDGMENT

This work was supported in part by the Natural Sciences and Engineering Research Council of Canada.

APPENDIX A: $M(P_{^3\mathrm{H}},P_{^3\mathrm{He}},M_t)$ IN THE EPM

Using the Dirac representation of the γ matrices, $M(P_{^3\mathrm{H}},P_{^3\mathrm{He}},M_t)$ (up to a constant phase factor) can be written in the form below, which operates on the product space of the leptonic and hadronic spinors,

[7]This already takes into account the fact that they took the value of $C=0.965$, while $C=0.9788$ is used in this work.

$$M(P_{^3\mathrm{H}},P_{^3\mathrm{He}},M_t)=\mathrm{N}'(1-\vec{\sigma}_L\cdot\hat{\nu})\Bigg\{f_1\vec{\sigma}_L\cdot\vec{\epsilon}_\lambda+f_2\vec{\sigma}\cdot\vec{\epsilon}_\lambda+if_3\vec{\epsilon}_\lambda\times\vec{\sigma}_L\cdot\vec{\sigma}+\frac{f_4}{2m}\vec{\sigma}_L\cdot\vec{\epsilon}_\lambda\vec{\sigma}\cdot\vec{s}$$
$$+\frac{f_6}{2m}\vec{\nu}\cdot\vec{\epsilon}_\lambda+i\frac{f_7}{2m}\vec{s}\times\vec{\epsilon}_\lambda\cdot\vec{\sigma}+\frac{f_8}{2m}\vec{\sigma}_L\cdot\vec{s}\vec{\sigma}\cdot\vec{\epsilon}_\lambda+\frac{f_9}{2m}\vec{\sigma}_L\cdot\vec{\sigma}\vec{\nu}\cdot\vec{\epsilon}_\lambda+\frac{f_{10}}{4m^2}\vec{\sigma}\cdot\vec{s}\vec{\nu}\cdot\vec{\epsilon}_\lambda+i\frac{f_{11}}{4m^2}\vec{s}\times\vec{\nu}\cdot\vec{\sigma}\vec{\sigma}_L\cdot\vec{\epsilon}_\lambda$$
$$+\frac{f_{12}}{4m^2}\vec{\sigma}\cdot\vec{\nu}\vec{\nu}\cdot\vec{\epsilon}_\lambda+\frac{f_{13}}{2m}\vec{\sigma}\cdot\vec{\nu}\vec{\sigma}_L\cdot\vec{\epsilon}_\lambda+i\frac{f_{14}}{4m^2}\vec{s}\times\vec{\epsilon}_\lambda\cdot\vec{\sigma}\vec{\sigma}_L\cdot\vec{s}+i\frac{f_{15}}{8m^3}\vec{s}\times\vec{\nu}\cdot\vec{\sigma}\vec{\nu}\cdot\vec{\epsilon}_\lambda\Bigg\}, \tag{A1}$$

where $\vec{\sigma}_L$ is the leptonic spin matrix and $\vec{\sigma}$ is the hadronic spin matrix. N' is the spinor normalization factor, which equals $\frac{1}{2}\sqrt{(P^0_{^3\mathrm{H}}+M_t)/2P^0_{^3\mathrm{He}}}$(the factor $\frac{1}{2}$ comes from the normalizations of the photon and the neutrino). The infrared divergent part comes from $1/\zeta$, where

$$\frac{1}{\zeta}=\frac{1}{2(P^0_{^3\mathrm{H}}k+k^2+\vec{\nu}\cdot\vec{k})},$$

a term of $\mathcal{O}(1/k)$.

$$f_1=\frac{F_V^H}{P^0_{^3\mathrm{H}}+M_t}\Bigg\{-\Bigg(1+\frac{k}{M_t}+\frac{P^0_{^3\mathrm{H}}}{M_t}+\frac{M_t\,k+k^2+2\vec{\nu}\cdot\vec{k}+P^0_{^3\mathrm{H}}k}{\zeta}\Bigg)+\lambda\Bigg(\frac{\nu}{M_t}-\frac{\nu k}{\zeta}\Bigg)-\kappa_i\frac{k-\lambda\nu}{2M_t}$$
$$+\kappa_f\Bigg[\frac{k}{2M_t}\frac{2kP^0_{^3\mathrm{H}}-2\vec{\nu}\cdot\vec{k}}{\zeta}-\lambda\Bigg(\frac{\nu k^2+P^0_{^3\mathrm{H}}\nu k}{M_t\zeta}\Bigg)\Bigg]\Bigg\}+F_V^L\Bigg\{\frac{1}{2}(\lambda-1)\frac{1}{m}\Bigg(1+\frac{\nu+k}{P^0_{^3\mathrm{H}}+M_t}\Bigg)\Bigg\}$$
$$+\frac{F_V'}{P^0_{^3\mathrm{H}}+M_t}\Bigg\{2(\nu^2-s^2+\vec{\nu}\cdot\vec{k})-2(P^0_{^3\mathrm{H}}+M_t)k+(\kappa_i-\kappa_f)\frac{\lambda\nu k^2+k\vec{\nu}\cdot\vec{k}}{M_t}\Bigg\}$$
$$+\frac{F_M^H}{P^0_{^3\mathrm{H}}+M_t}\Bigg\{(\lambda+1)\frac{\nu}{2M_t}\Bigg(1+\frac{\nu}{M_t}\Bigg)+\Bigg(\frac{P^0_{^3\mathrm{H}}-k}{2M_t}\Bigg)\Bigg(\frac{\nu-m}{M_t}\Bigg)-\frac{k(\nu-m)}{2\zeta}+\frac{\lambda\nu}{2M_t}\Bigg(\frac{P^0_{^3\mathrm{H}}-k-m}{M_t}\Bigg)$$
$$-\frac{m}{2M_t}\Bigg(1+\frac{-P^0_{^3\mathrm{H}}k-2\vec{\nu}\cdot\vec{k}-k^2}{\zeta}\Bigg)-\frac{\nu}{2M_t}\frac{2\vec{\nu}\cdot\vec{k}-(1-\lambda)\nu k+(\lambda+1)(P^0_{^3\mathrm{H}}k+k^2)}{\zeta}-\frac{\lambda\nu k}{2\zeta}\Bigg(1-\frac{m}{M_t}\Bigg)$$
$$+\frac{\lambda\kappa_i\nu}{4M_t}\Bigg(1+\frac{P^0_{^3\mathrm{H}}+\nu-m}{M_t}\Bigg)+\frac{\kappa_i(m-\nu)k}{4M_t^2}+\kappa_f\Bigg[-\frac{\lambda\nu k^2}{2M_t\zeta}\Bigg(1+\frac{P^0_{^3\mathrm{H}}+\nu-m}{M_t}\Bigg)+\frac{mk}{4\zeta}\Bigg(1-\frac{P^{0\,2}_{^3\mathrm{H}}}{M_t^2}+\frac{2\vec{\nu}\cdot\vec{k}-s^2-2P^0_{^3\mathrm{H}}k}{M_t^2}\Bigg)$$
$$-\frac{\nu k}{4\zeta}\Bigg(1-\frac{2\nu}{M_t}-\frac{2(P^0_{^3\mathrm{H}}k+\nu k-\vec{\nu}\cdot\vec{k}+\nu P^0_{^3\mathrm{H}})+s^2+P^{0\,2}_{^3\mathrm{H}}}{M_t^2}\Bigg)-\frac{\lambda\nu k}{4\zeta}\Bigg(1+\frac{2P^0_{^3\mathrm{H}}}{M_t}+\frac{2(P^0_{^3\mathrm{H}}\nu-P^0_{^3\mathrm{H}}m-\vec{\nu}\cdot\vec{k})+P^{0\,2}_{^3\mathrm{H}}+s^2}{M_t^2}\Bigg)\Bigg]\Bigg\}$$
$$+\frac{F_M^L}{P^0_{^3\mathrm{H}}+M_t}\Bigg\{(\lambda-1)\Bigg(-\frac{\nu+k}{4M_t}+\frac{(\nu+k)^2-s^2}{4mM_t}\Bigg)\Bigg\}+\frac{F_M'}{P^0_{^3\mathrm{H}}+M_t}\Bigg\{\frac{m-\nu}{M_t}(\vec{\nu}\cdot\vec{k}+\lambda\nu k)\Bigg\}$$
$$+\frac{F_A^H}{P^0_{^3\mathrm{H}}+M_t}\Bigg\{-\lambda\Bigg[1+\frac{P^0_{^3\mathrm{H}}+k}{M_t}\Bigg(1-\frac{M_t\,k}{\zeta}\Bigg)-\frac{M_t\,k}{\zeta}\Bigg]+\frac{\nu}{M_t}-\frac{k\nu}{\zeta}-\frac{\lambda\kappa_i}{2}\Bigg(1+\frac{P^0_{^3\mathrm{H}}}{M_t}\Bigg)$$
$$+\lambda\kappa_f\Bigg(\frac{2k(P^0_{^3\mathrm{H}}+k)+M_tk}{2\zeta}+\frac{P^0_{^3\mathrm{H}}}{2M_t}\frac{k(2k+P^0_{^3\mathrm{H}})}{\zeta}+\frac{k}{2M_t}\frac{s^2-2\vec{\nu}\cdot\vec{k}}{\zeta}\Bigg)-\kappa_f\Bigg(\frac{k}{2M_t}\frac{2\nu(P^0_{^3\mathrm{H}}+k)}{\zeta}+\frac{k\nu}{\zeta}\Bigg)\Bigg\},$$

$$f_2=\frac{F_V^H}{P_{^3\mathrm{H}}^0+M_t}\left\{-\frac{\lambda(2+\kappa_i)}{2}\left(1+\frac{P_{^3\mathrm{H}}^0}{M_t}\right)+\frac{\lambda k(M_t+P_{^3\mathrm{H}}^0)}{\zeta}+\lambda\kappa_f\left[\left(1+\frac{P_{^3\mathrm{H}}^0}{2M_t}\right)\frac{P_{^3\mathrm{H}}^0 k}{\zeta}+\frac{M_t k}{2\zeta}+\frac{ks^2}{2M_t\zeta}\right]\right\}$$
$$+F_V'\left\{\lambda(\kappa_i-\kappa_f)k\left(\frac{\nu+k}{M_t}\right)\right\}+\frac{F_M^H}{P_{^3\mathrm{H}}^0+M_t}\left\{-\frac{k}{2M_t}\left(1+\frac{P_{^3\mathrm{H}}^0}{M_t}+\frac{M_t k}{\zeta}\right)+\frac{2\lambda+\kappa_i}{4}\left[-\frac{k}{M_t}\left(1+\frac{P_{^3\mathrm{H}}^0}{M_t}\right)\right]+\frac{\lambda(2+\kappa_i)}{4}\frac{s^2}{M_t^2}\right.$$
$$+\lambda\left(\frac{M_t k-k^2}{2\zeta}+\frac{k}{M_t}\frac{2s^2-P_{^3\mathrm{H}}^{0\,2}-(1+\lambda)P_{^3\mathrm{H}}^0 k}{2\zeta}\right)+\kappa_f\left\{\frac{\lambda k}{4M_t}\left[\frac{s^2}{\zeta}\left(1-\frac{P_{^3\mathrm{H}}^0-k}{M_t}\right)-\frac{\vec{\nu}\cdot\vec{k}+\nu^2}{\zeta}\left(1+\frac{P_{^3\mathrm{H}}^0}{M_t}\right)\right]\right.$$
$$\left.\left.-\frac{k^2}{4\zeta}\left[1+\frac{P_{^3\mathrm{H}}^0}{M_t}\left(2+\frac{P_{^3\mathrm{H}}^0}{M_t}\right)+\lambda\left(1-\frac{P_{^3\mathrm{H}}^{0\,2}}{M_t^2}\right)\right]\right\}\right\}+\frac{F_A^H}{P_{^3\mathrm{H}}^0+M_t}\left\{-1-\frac{P_{^3\mathrm{H}}^0}{M_t}-\frac{(P_{^3\mathrm{H}}^0+M_t)k}{\zeta}+\kappa_f\left(\frac{k}{2M_t}\frac{P_{^3\mathrm{H}}^{0\,2}+s^2}{\zeta}\right.\right.$$
$$\left.\left.-\frac{M_t k}{\zeta}\right)\right\}+F_A^L\left\{\frac{\lambda-1}{2m}\right\}+F_A'\{-2(\nu+k)\}+\frac{F_P^H}{P_{^3\mathrm{H}}^0+M_t}\left\{\left(-1-\frac{P_{^3\mathrm{H}}^0}{M_t}+\frac{(M_t+P_{^3\mathrm{H}}^0)k}{\zeta}\right)+\kappa_f\left[\frac{k}{2M_t}\left(-\frac{P_{^3\mathrm{H}}^{0\,2}+s^2}{\zeta}\right)+\frac{M_t k}{\zeta}\right]\right\},$$

$$f_3=\frac{F_V^H}{P_{^3\mathrm{H}}^0+M_t}\left\{1+\frac{P_{^3\mathrm{H}}^0}{M_t}-\frac{(M_t+P_{^3\mathrm{H}}^0)k}{\zeta}+\kappa_f\left[-\frac{M_t k}{2\zeta}+\frac{k}{2M_t}\left(\frac{P_{^3\mathrm{H}}^{0\,2}+s^2}{\zeta}\right)\right]\right\}$$
$$+\frac{F_M^H}{P_{^3\mathrm{H}}^0+M_t}\left\{\frac{2m-[2+\lambda(2+\kappa_i)]\nu}{4M_t}\left(1+\frac{P_{^3\mathrm{H}}^0}{M_t}\right)+\frac{k[m-(1+\lambda)\nu]}{2\zeta}\left(1+\frac{P_{^3\mathrm{H}}^0}{M_t}\right)+\kappa_f\frac{k(\nu-m)}{4\zeta}\left(\frac{s^2+P_{^3\mathrm{H}}^{0\,2}}{M_t^2}-1\right)\right.$$
$$\left.-\lambda\kappa_f\frac{k\nu}{4\zeta}\left(1+\frac{P_{^3\mathrm{H}}^0}{M_t}\right)^2\right\}+F_M^L\left\{\frac{1}{2M_t}\right\}+\frac{F_A^H}{P_{^3\mathrm{H}}^0+M_t}\left\{\frac{\lambda(2+\kappa_i)}{2}\left(1+\frac{P_{^3\mathrm{H}}^0}{M_t}\right)+\lambda\left(\frac{k(M_t+P_{^3\mathrm{H}}^0)}{\zeta}\right)\right.$$
$$\left.+\lambda\kappa_f\left(\frac{k(M_t+2P_{^3\mathrm{H}}^0)}{2\zeta}+\frac{k}{M_t}\frac{P_{^3\mathrm{H}}^{0\,2}+s^2}{2\zeta}\right)\right\}+F_A^L\left\{\frac{\lambda-1}{2m}\right\},$$

$$f_4=\frac{F_V^H}{P_{^3\mathrm{H}}^0+M_t}\left\{\lambda(2+\kappa_i)\frac{m}{M_t}-\frac{2\lambda mk}{\zeta}\left(1-\kappa_f\frac{P_{^3\mathrm{H}}^0}{M_t}\right)\right\}$$
$$+\frac{F_M^H}{P_{^3\mathrm{H}}^0+M_t}\left\{\lambda(2+\kappa_i)\frac{m(\nu-m)}{2M_t^2}+\lambda\frac{m(m-\nu)}{\zeta}\frac{k}{M_t}+\frac{m\nu}{M_t^2}+\lambda\kappa_f\frac{m(\nu-m)}{M_t^2}\frac{P_{^3\mathrm{H}}^0 k}{\zeta}\right\}$$
$$+\frac{F_A^H}{P_{^3\mathrm{H}}^0+M_t}\left\{\frac{2m}{M_t}\left(1+\frac{M_t k}{\zeta}\right)+\kappa_f\frac{2m}{M_t}\frac{(P_{^3\mathrm{H}}^0+M_t)k}{\zeta}\right\}+F_A^L\left\{\frac{1-\lambda}{P_{^3\mathrm{H}}^0+M_t}\right\}+F_A'\left\{4m+\frac{4mk}{P_{^3\mathrm{H}}^0+M_t}\right\}+F_P^L\left\{\frac{\lambda+1}{P_{^3\mathrm{H}}^0+M_t}\right\},$$

$$f_6=\frac{F_V^H}{P_{^3\mathrm{H}}^0+M_t}\left\{\frac{2m}{M_t}\left(1+\frac{\lambda}{2}(2+\kappa_i)\right)+(1-\lambda)\frac{2mk}{\zeta}+\frac{4m(P_{^3\mathrm{H}}^0+M_t+\nu)}{\zeta}+\kappa_f\frac{2m}{M_t}\frac{k\nu-\lambda(P_{^3\mathrm{H}}^0 k+k^2)}{\zeta}\right\}$$
$$+\frac{F_V'}{P_{^3\mathrm{H}}^0+M_t}\left\{4m(\nu+k+M_t+P_{^3\mathrm{H}}^0)-(1+\lambda)(\kappa_f-\kappa_i)\frac{2mk^2}{M_t}\right\}$$
$$+\frac{F_M^H}{P_{^3\mathrm{H}}^0+M_t}\left\{(1+\lambda)\frac{m}{M_t}\left(1+\frac{\nu-k+P_{^3\mathrm{H}}^0}{M_t}-\frac{k^2}{\zeta}\right)+\frac{m(M_t-k)}{\zeta}\right.$$
$$\left.+\frac{m}{M_t}\left(\frac{\lambda k(m-\nu-M_t-P_{^3\mathrm{H}}^0)}{\zeta}+\frac{k\nu-2m\nu-kP_{^3\mathrm{H}}^0+s^2-2\vec{\nu}\cdot\vec{k}-P_{^3\mathrm{H}}^{0\,2}}{\zeta}\right)-\lambda\frac{m^2}{M_t^2}\right.$$

$$+\lambda\kappa_i\frac{m}{2M_t}\left(1+\frac{P^0_{^3\mathrm{H}}+\nu-m}{M_t}\right)-\kappa_i\frac{m}{2M_t}\frac{k}{M_t}-\kappa_f\frac{mk}{2\zeta}\left(1-\frac{2\nu}{M_t}+\frac{2m\nu-2k\nu-2P^0_{^3\mathrm{H}}k-P^{0\,2}_{^3\mathrm{H}}+2\vec{\nu}\cdot\vec{k}-s^2-2P^0_{^3\mathrm{H}}\nu}{M_t^2}\right)$$

$$+\lambda\kappa_f\left\{-\frac{mk}{2\zeta}\left[\left(1+\frac{P^0_{^3\mathrm{H}}}{M_t}\right)^2-\frac{2\vec{\nu}\cdot\vec{k}-s^2-2P^0_{^3\mathrm{H}}k-2\nu k+2mk+2mP^0_{^3\mathrm{H}}-2\nu P^0_{^3\mathrm{H}}}{M_t^2}+\frac{2k}{M_t}\right]\right\}$$

$$+F_M^L\left\{\frac{1}{P^0_{^3\mathrm{H}}+M_t}\frac{m}{M_t}\right\}+\frac{F'_M}{P^0_{^3\mathrm{H}}+M_t}\left\{-\frac{2m}{M_t}(\vec{\nu}\cdot\vec{k}+m\nu)+\lambda\frac{2mk}{M_t}(m-\nu)\right\}$$

$$+\frac{F_A^H}{P^0_{^3\mathrm{H}}+M_t}\left\{(1+\lambda)\left(\frac{2m}{M_t}-(1+\kappa_f)\frac{2mk}{\zeta}\right)+\lambda\kappa_i\frac{m}{M_t}-\kappa_f\left(\frac{2m}{M_t}\frac{k^2+kP^0_{^3\mathrm{H}}}{\zeta}-\frac{2\lambda m}{M_t}\frac{\nu k}{\zeta}\right)\right\}$$

$$+\frac{F_P^H}{P^0_{^3\mathrm{H}}+M_t}\left\{-\lambda\frac{m}{M_t}(2+\kappa_i)+(\kappa_f+1)\lambda\frac{2mk}{\zeta}\right\},$$

$$f_7=\frac{F_V^H}{P^0_{^3\mathrm{H}}+M_t}\left\{\frac{2m}{M_t}+\frac{2mk}{\zeta}\left[1+\kappa_f\left(1+\frac{P^0_{^3\mathrm{H}}}{M_t}\right)\right]\right\}+F_V^L\left\{\frac{1-\lambda}{P^0_{^3\mathrm{H}}+M_t}\right\}+\frac{F'_V}{P^0_{^3\mathrm{H}}+M_t}\left\{4m(\nu+k)+2(\kappa_i-\kappa_f)\frac{k}{M_t}m(\nu+k)\right\}$$

$$+\frac{F_M^H}{P^0_{^3\mathrm{H}}+M_t}\left\{(1+\lambda)\left(\frac{m}{M_t}+\frac{mk}{\zeta}\right)\left(1+\frac{P^0_{^3\mathrm{H}}}{M_t}\right)-\frac{2+\kappa_i}{2}\frac{m}{M_t}\frac{k}{M_t}-\frac{mM_t}{\zeta}\left(1-\frac{P^{0\,2}_{^3\mathrm{H}}-s^2-k^2}{M_t^2}\right)\right.$$

$$\left.+\frac{\kappa_f}{2}\frac{mk}{\zeta}\left(1-\frac{k}{M_t}-\frac{P^0_{^3\mathrm{H}}(P^0_{^3\mathrm{H}}-k)+s^2}{M_t^2}\right)+\frac{\kappa_f\lambda}{2}\frac{mk}{\zeta}\left(1+\frac{P^0_{^3\mathrm{H}}}{M_t}\right)^2+\kappa_i\lambda\frac{m}{2M_t}\left(1+\frac{P^0_{^3\mathrm{H}}}{M_t}\right)\right\}$$

$$+\frac{F_M^L}{P^0_{^3\mathrm{H}}+M_t}\left\{\frac{1-\lambda}{2}\left(1+\frac{P^0_{^3\mathrm{H}}+\nu+k}{M_t}\right)+(\lambda+1)\frac{m}{2M_t}\right\}+\frac{F_A^H}{P^0_{^3\mathrm{H}}+M_t}\left\{\lambda(2+\kappa_i)\frac{m}{M_t}+\lambda\left[-\frac{2mk}{\zeta}\left(1-\frac{\kappa_f P^0_{^3\mathrm{H}}}{M_t}\right)\right]\right\}$$

$$+\frac{F_P^H}{P^0_{^3\mathrm{H}}+M_t}\left\{-\lambda\frac{m}{M_t}(2+\kappa_i)+\lambda\frac{2mk}{\zeta}\left(1-\frac{\kappa_f P^0_{^3\mathrm{H}}}{M_t}\right)\right\},$$

$$f_8=\frac{F_V^H}{P^0_{^3\mathrm{H}}+M_t}\left\{\lambda\frac{m}{M_t}(2+\kappa_i)+\lambda\frac{2mk}{\zeta}\left(1-\frac{\kappa_f P^0_{^3\mathrm{H}}}{M_t}\right)\right\}+F_V^L\left\{\frac{\lambda-1}{P^0_{^3\mathrm{H}}+M_t}\right\}+F'_V\left\{\frac{2mk\lambda(\kappa_i-\kappa_f)}{P^0_{^3\mathrm{H}}+M_t}\left(1+\frac{P^0_{^3\mathrm{H}}}{M_t}\right)\right\}$$

$$+\frac{F_M^H}{P^0_{^3\mathrm{H}}+M_t}\left\{\lambda\frac{\nu-m}{4M_t}\left(\frac{2m(2+\kappa_i)}{M_t}+\frac{4mk}{\zeta}\right)+\lambda\kappa_f\frac{mk}{\zeta}\frac{P^0_{^3\mathrm{H}}(m-\nu)}{M_t^2}\right\}$$

$$+F_M^L\left\{\frac{1-\lambda}{4(P^0_{^3\mathrm{H}}+M_t)}\left[-2+\frac{2m}{M_t}\left(1-\frac{P^0_{^3\mathrm{H}}+\nu+k}{m}\right)\right]\right\}+\frac{F_A^H}{P^0_{^3\mathrm{H}}+M_t}\left\{\left(\frac{2m}{M_t}-\frac{2mk}{\zeta}\right)-\kappa_f\frac{2mk}{\zeta}\left(1+\frac{P^0_{^3\mathrm{H}}}{M_t}\right)\right\}+F'_A\{-4m\},$$

$$f_9=\frac{F_V^H}{P^0_{^3\mathrm{H}}+M_t}\left\{-\lambda(2+\kappa_i)\frac{m}{M_t}-\frac{2mk}{\zeta}(\lambda+2\hat{\nu}\cdot\hat{k})-\frac{4m\nu}{\zeta}-\kappa_f\frac{2mk}{\zeta}\left(\lambda+\frac{\hat{\nu}\cdot\vec{k}+\nu}{M_t}\right)\right\}+F_V^L\left\{\frac{1-\lambda}{P^0_{^3\mathrm{H}}+M_t}\right\}$$

$$+F_V'\left\{-4m\frac{\nu+\hat{\nu}\cdot\vec{k}}{P^0_{^3\mathrm{H}}+M_t}\right\}+\frac{F_M^H}{P^0_{^3\mathrm{H}}+M_t}\left\{-(1+\lambda)\frac{m\nu}{M_t^2}+\lambda\frac{m^2}{M_t^2}+\frac{m\nu}{\zeta}\left(\frac{k}{M_t}-4\right)+\frac{\lambda mk}{\zeta}\frac{m-\nu-k}{M_t}+\frac{\vec{\nu}\cdot\vec{k}}{\zeta}\left[-\frac{2m}{M_t}\left(1-\frac{m}{\nu}\right)\right]\right.$$

$$\left.-\frac{m\hat{\nu}\cdot\vec{k}}{M_t^2}+\lambda\kappa_i\frac{m(m-\nu)}{2M_t^2}+\kappa_f\frac{mk}{\zeta}\frac{m\nu-\nu^2+\vec{\nu}\cdot\hat{k}(m-k)}{M_t^2}+\lambda\kappa_f\frac{mk}{\zeta}\left(\frac{m-\nu-k}{M_t}-\frac{s^2-2\nu^2-2\vec{\nu}\cdot\vec{k}+2P^0_{^3\mathrm{H}}k}{2M_t^2}\right)\right\}$$

$$+\frac{F_M^L(1-\lambda)}{P^0_{^3\mathrm{H}}+M_t}\left\{\frac{1}{2}\left(1+\frac{P^0_{^3\mathrm{H}}}{M_t}\right)-\frac{m}{2M_t}+\frac{k+\nu}{2M_t}\right\}+\frac{F_M'}{P^0_{^3\mathrm{H}}+M_t}\left\{-2m\nu\left(1-\frac{m-\nu-\hat{\nu}\cdot\vec{k}-P^0_{^3\mathrm{H}}}{M_t}\right)+\frac{2m^2\hat{\nu}\cdot\vec{k}}{M_t}\right\}$$

$$+\frac{F_A^H}{P^0_{^3\mathrm{H}}+M_t}\left\{-\frac{2m}{M_t}\left(1-\frac{M_t k}{\zeta}\right)-\kappa_f\lambda\frac{2mk}{\zeta}\left(\frac{\nu+\hat{\nu}\cdot\vec{k}}{M_t}\right)+\frac{4m(P^0_{^3\mathrm{H}}+M_t)}{\zeta}\right\}+F_A'\{4m\},$$

$$f_{10}=\frac{F_V^H}{P^0_{^3\mathrm{H}}+M_t}\left\{-\frac{4\kappa_f\lambda m^2}{\zeta}\frac{k}{M_t}\right\}+\frac{F_M^H}{P^0_{^3\mathrm{H}}+M_t}\left\{\frac{2m^2}{M_t^2}+\lambda\frac{4m^2}{\zeta}\frac{k}{M_t}\left(-1+\kappa_f\frac{3P^0_{^3\mathrm{H}}}{4M_t}-\frac{\kappa_f}{4}\right)\right\}+\frac{F_A^H}{P^0_{^3\mathrm{H}}+M_t}\left\{-\frac{4m^2}{\zeta}\left(2+\kappa_f\frac{k}{M_t}\right)\right\}$$

$$+\frac{F_A'}{P^0_{^3\mathrm{H}}+M_t}\left\{-8m^2+\frac{16M_t m^3(1+\varepsilon)}{m_\pi^2-Q_L^2}\right\}+\frac{F_P^H}{P^0_{^3\mathrm{H}}+M_t}\left\{\frac{8m^2}{\zeta}+\frac{8m^2}{m_\pi^2-Q_L^2}+\kappa_f\frac{4m^2}{\zeta}\frac{k}{M_t}\right\},$$

$$f_{11}=\frac{F_V'}{P^0_{^3\mathrm{H}}+M_t}\{8m^2\}+\frac{F_M^H}{P^0_{^3\mathrm{H}}+M_t}\left\{\frac{2m^2}{M_t^2}\right\},$$

$$f_{12}=\frac{F_V^H}{P^0_{^3\mathrm{H}}+M_t}\left\{\frac{8m^2}{\zeta}\left(\lambda\frac{k}{\nu}-1\right)+\kappa_f\frac{4m^2}{\zeta}\frac{k}{M_t}\left(\lambda\frac{k}{\nu}-1\right)\right\}+\frac{F_V'}{P^0_{^3\mathrm{H}}+M_t}\left\{8m^2\left(\lambda\frac{k}{\nu}-1\right)\right\}$$

$$+\frac{F_M^H}{P^0_{^3\mathrm{H}}+M_t}\left\{\frac{2m^2}{M_t^2}\left(\lambda\frac{k}{\nu}-1\right)-\frac{8m^2}{\zeta}+\frac{4\lambda m^2}{\zeta}\frac{k}{M_t}\left(1-\frac{m}{\nu}\right)-\kappa_f\frac{4m^2}{\zeta}\frac{k}{M_t}+\lambda\kappa_f\frac{2m^2}{\zeta}\frac{k}{M_t}\left[-\frac{1}{2}+\frac{k}{M_t}\left(1-\frac{m}{\nu}\right)\right.\right.$$

$$\left.\left.+\frac{2\nu-P^0_{^3\mathrm{H}}}{2M_t}\right]\right\}+\frac{F_M'}{P^0_{^3\mathrm{H}}+M_t}\left\{-4m^2\left(1-\frac{m-\nu-P^0_{^3\mathrm{H}}}{M_t}\right)+4\lambda m^2\frac{k}{M_t}\left(1-\frac{m}{\nu}\right)\right\}+\frac{F_A^H}{P^0_{^3\mathrm{H}}+M_t}\left\{\kappa_f\frac{4m^2}{\zeta}\frac{k}{M_t}\left(-\lambda+\frac{k}{\nu}\right)\right\},$$

$$f_{13}=\frac{F_V^H}{P^0_{^3\mathrm{H}}+M_t}\left\{\frac{4mk}{\zeta}\left(1+\kappa_f\frac{k}{M_t}\right)(\lambda+\hat{\nu}\cdot\hat{k})\right\}+\frac{F_V'}{P^0_{^3\mathrm{H}}+M_t}\{4mk(\lambda+\hat{\nu}\cdot\hat{k})\}+\frac{F_M^H}{P^0_{^3\mathrm{H}}+M_t}\left\{\frac{m\hat{\nu}\cdot\vec{k}}{M_t^2}+\frac{2mk}{\zeta}\left(\frac{2\hat{\nu}\cdot\hat{k}(\nu-m)-k}{2M_t}\right)\right.$$

$$\left.+\frac{\lambda mk}{M_t^2}+\frac{2\lambda mk}{\zeta}\left(\frac{2(\nu-m)+k}{2M_t}\right)+\kappa_f\frac{2mk}{\zeta}\left(\frac{2[(\lambda-1)(\nu k-\vec{\nu}\cdot\vec{k})-2P^0_{^3\mathrm{H}}(\nu-\lambda k)-2m(\hat{\nu}\cdot\vec{k}+\lambda k)]+\lambda s^2}{4M_t^2}+\frac{\lambda k-\nu}{2M_t}\right)\right\}$$

$$+\frac{F_M'}{P^0_{^3\mathrm{H}}+M_t}\left\{\frac{2m}{M_t}[\hat{\nu}\cdot\hat{k}(\nu k-mk)-\lambda k(m-\nu)]\right\}+\frac{F_A^H}{P^0_{^3\mathrm{H}}+M_t}\left\{\kappa_f\frac{2mk}{\zeta}\frac{k}{M_t}(1+\lambda\hat{\nu}\cdot\hat{k})\right\}+F_A'\{-4m\},$$

$$f_{14}=\frac{F_V'}{P^0_{^3\mathrm{H}}+M_t}\left\{8m^2+(\kappa_i-\kappa_f)\frac{4m^2k}{M_t}\right\},$$

TABLE II. Some important quantities of trinucleon wave functions. The binding energy E_b is in MeV. $P(S)$ denotes the probability of S-wave component of the wave function and so on.

Potential	E_b	$P(S)$	$P(S')$	$P(P)$	$P(D)$	$\langle\psi\|\psi\rangle_{\rm num}$
Bonn A	8.29	92.59%	1.23%	0.030%	6.14%	0.994
Bonn B	8.10	91.61%	1.19%	0.044%	7.16%	0.993
CD Bonn (^{3}He)	7.91	91.61%	1.35%	0.041%	7.01%	0.993
CD Bonn (^{3}H)	7.96	91.63%	1.31%	0.041%	7.01%	0.993
Nijmegen I	7.66	90.31%	1.29%	0.065%	8.34%	0.990
Paris	7.38	90.11%	1.40%	0.069%	8.42%	0.988
AV14	7.58	89.86%	1.15%	0.082%	8.90%	0.987

$$f_{15}=\frac{F_V^H}{P^0_{^3\mathrm{H}}+M_\mathrm{t}}\left\{\frac{16m^3}{\zeta\nu}\left(1+\kappa_f\frac{k}{2M_\mathrm{t}}\right)\right\}+F_V'\left\{\frac{16m^3}{(P^0_{^3\mathrm{H}}+M_\mathrm{t})\nu}\right\}$$
$$+\frac{F_M^H}{P^0_{^3\mathrm{H}}+M_\mathrm{t}}\left\{\frac{4m^3}{M_\mathrm{t}^2\nu}\left[1-\left(2+\kappa_f\frac{k}{M_\mathrm{t}}\right)\frac{M_\mathrm{t}m}{\zeta}\right]\right\}$$
$$+F_M'\left\{-\frac{8m^4}{M_\mathrm{t}(P^0_{^3\mathrm{H}}+M_\mathrm{t})\nu}\right\}+F_A^H\left\{\kappa_f\frac{8m^3\lambda k}{M_\mathrm{t}(P^0_{^3\mathrm{H}}+M_\mathrm{t})\zeta\nu}\right\}. \quad \text{(A2)}$$

APPENDIX B: WAVE FUNCTION CHARACTERISTICS

Table II lists several important quantities that depend on the potential used to generate the wave function. They are, respectively, the binding energy given by the wave functions, various partial wave probabilities, and the numerical normalization $\langle\psi|\psi\rangle_{\rm num}$ of the wave functions. The numerical normalizations of all the wave functions are not unity because the antisymmetrization of the wave functions is projected on a finite set of states. The experimental binding energy E_b of ^{3}He is 7.72 MeV and of ^{3}H is 8.48 MeV [31].

[1] D. H. Wright, TRIUMF research proposal E592, 1990.
[2] D. H. Wright *et al.*, Few-Body Syst., Suppl. **12**, 275 (2000).
[3] N. C. Mukhopadhyay, Phys. Rep. **30**, 1 (1977).
[4] D. F. Measday, Phys. Rep. **354**, 243 (2001).
[5] L. Klieb and H. P. C. Rood, Nucl. Phys. **A356**, 483 (1981).
[6] L. Klieb, Ph.D. thesis, University of Groningen, The Netherlands, 1982.
[7] J. G. Congleton, Ph.D. thesis, University of British Columbia, 1992.
[8] J. G. Congleton and H. W. Fearing, Nucl. Phys. **A552**, 534 (1993).
[9] J. G. Congleton and E. Truhlik, Phys. Rev. C **53**, 956 (1996).
[10] J. Govaerts and J-L. Lucio-Martinez, Nucl. Phys. **A678**, 110 (2000).
[11] S. L. Adler and Y. Dothan, Phys. Rev. **151**, 1267 (1966).
[12] H. P. C. Rood and H. A. Tolhoek, Nucl. Phys. **70**, 658 (1965).
[13] P. Christillin and S. Servadio, Nuovo Cimento **42**, 165 (1977).
[14] H. Primakoff, Nucl. Phys. **A317**, 219 (1979).
[15] C. W. Kim and H. Primakoff, Phys. Rev. **140**, B566 (1965).
[16] C. W. Kim and H. Primakoff, Phys. Rev. **139**, B1447 (1965).
[17] H. W. Fearing, Phys. Rev. C **21**, 1951 (1980).
[18] L. Klieb, Nucl. Phys. **A442**, 721 (1985).
[19] Particle Data Group, D. E. Groom *et al.*, Eur. Phys. J. C **15**, 1 (2000).
[20] W. Schadow, W. Sandhas, J. Haidenbauer, and A. Nogga, Few-Body Syst. **28**, 241 (2000).
[21] W. Schadow, Ph.D. thesis, Bonn University, Germany, 1997.
[22] W. Glöckle, *The Quantum Mechanical Few Body Problem* (Springer-Verlag, Berlin, 1983).
[23] G. B. Arfken and H. J. Weber, *Mathematical Methods for Physicists* (Academic, New York, 1995).
[24] D. M. Brink and G. R. Satchler, *Angular Momentum* (Oxford Science, New York, 1993).
[25] J. Delorme, in *Mesons in Nuclei*, edited by M. Rho and D. H. Wilkinson (North-Holland, Amsterdam, 1979), Vol. I, p. 107.
[26] E. A. Peterson, Phys. Rev. **167**, 971 (1968).
[27] A. D. Lahiff and I. R. Afnan, Phys. Rev. C **56**, 2387 (1997).
[28] P. Ackerbauer *et al.*, Phys. Lett. B **417**, 224 (1998).
[29] H. Kameyama, M. Kamimura, and Y. Fukushima, Phys. Rev. C **40**, 974 (1989).
[30] H. W. Fearing, Phys. Rev. Lett. **35**, 79 (1975).
[31] A. H. Wapstra and G. Audi, Nucl. Phys. **A595**, 409 (1995).